halogenated thymidines, indicating that these compounds impair the pathway by which DNA methylation is translated into histone deacetylation. Because *in vitro* experiments in this study showed that halogenated thymidines had no effect on the binding of the methyl-CpG binding domain with methylated DNA, they are considered to interfere with some steps downstream of MBDs. Further studies will be needed to clarify the antisilencing mechanism of these compounds.

The findings that halogenated thymidines have a different antisilencing mechanism from and show remarkable synergistic effects with 5-aza-dC raise possibilities that halogenated thymidines could become attractive lead compounds in treatments of cancers. Furthermore, this study implicates a new mechanism of halogenated thymidines that interfere with step(s) between DNA methylation and histone acetylation.

Acknowledgments

References

1. Bird AP, Wolffe AP. Methylation-induced repression—belts, braces, and chromatin. Cell 1999;99:451–4.
2. Jones PA, Laird PW. Cancer epigenetics comes of age. Nat Genet 1999;21:163–7.
3. Baylin SB, Herman JG. DNA hypermethylation in tumorigenesis: epigenetics joins genetics. Trends Genet 2000;16:168–74.
4. Jones PA, Baylin SB. The fundamental role of epigenetic events in cancer. Nat Rev Genet 2002;3: 415–28.
5. Egger G, Liang G, Aparicio A, Jones PA. Epigenetics in human disease and prospects for epigenetic therapy. Nature 2004;429:457–63.
6. Issa JP. Decitabine. Curr Opin Oncol 2003;15:446–51.
7. Ballestar E, Wolffe AP. Methyl-CpG-binding proteins. Targeting specific gene repression. Eur J Biochem 2001;268:1–6.
8. Slack A, Bovenzi V, Bigey P, et al. Antisense *MBD2* gene therapy inhibits tumorigenesis. J Gene Med 2002; 4:381–9.
9. Sansom OJ, Berger J, Bishop SM, Hendrich B, Bird A, Clarke AR. Deficiency of MBD2 suppresses intestinal tumorigenesis. Nat Genet 2003;34:145–7.
10. Christman JK. 5-Azacytidine and 5-aza-2'-deoxycytidine as inhibitors of DNA methylation: mechanistic studies and their implications for cancer therapy. Oncogene 2002;21:5483–95.
11. Kantarjian HM, O'Brien S, Cortes J, et al. Results of decitabine (5-aza-2'deoxycytidine) therapy in 130 patients with chronic myelogenous leukemia. Cancer 2003;98:522–8.
12. Goffin J, Eisenhauer E. DNA methyltransferase inhibitors—state of the art. Ann Oncol 2002;13: 1699–716.
13. Hurd PJ, Whitmarsh AJ, Baldwin GS, et al. Mechanism-based inhibition of C5-cytosine DNA methyltransferases by 2-*H* pyrimidinone. J Mol Biol 1999; 286:389–401.
14. Cheng JC, Matsen CB, Gonzales FA, et al. Inhibition of DNA methylation and reactivation of silenced genes by zebularine. J Natl Cancer Inst 2003;95:399–409.
15. Cheng JC, Weisenberger DJ, Gonzales FA, et al. Continuous zebularine treatment effectively sustains demethylation in human bladder cancer cells. Mol Cell Biol 2004;24:1270–8.

16. Satou Y, Nosaka K, Koya Y, Yasunaga JI, Toyokuni S, Matsuoka M. Proteasome inhibitor, bortezomib, potently inhibits the growth of adult T-cell leukemia cells both *in vivo* and *in vitro*. Leukemia 2004;18:1357–63.
17. Chou TC, Talalay P. Analysis of combined drug effects: a new look at a very old problem. Trends Pharmacol Sci 1983;4:450–4.
18. Chou J. Quantitation of synergism and antagonism of two or more drugs by computerized analysis. In: Chou TC, Rideout DC, editors. Synergism and antagonism in chemotherapy. San Diego (CA): Academic Press; 1991. p. 223–44.
19. Nosaka K, Maeda M, Tamiya S, Sakai T, Mitsuya H, Matsuoka M. Increasing methylation of the *CDKN2A* gene is associated with the progression of adult T-cell leukemia. Cancer Res 2000;60:1043–8.
20. Wang L, Groves MJ, Hepburn MD, Bowen DT. Glutathione *S*-transferase enzyme expression in hematopoietic cell lines implies a differential protective role for T1 and A1 isoenzymes in erythroid and for M1 in lymphoid lineages. Haematologica 2000;85:573–9.
21. Mutskov V, Felsenfeld G. Silencing of transgene transcription precedes methylation of promoter DNA and histone H3 lysine 9. EMBO J 2004;23:138–49.
22. Ohki I, Shimotake N, Fujita N, et al. Solution structure of the methyl-CpG binding domain of human MBD1 in complex with methylated DNA. Cell 2001; 105:487–97.
23. Fraga MF, Ballestar E, Montoya G, Taysavang P, Wade PA, Esteller M. The affinity of different MBD proteins for a specific methylated locus depends on their intrinsic binding properties. Nucleic Acids Res 2003;31:1765–74.
24. Hino S, Fan J, Taguwa S, Akasaka K, Matsuoka M. Sea urchin insulator protects lentiviral vector from silencing by maintaining active chromatin structure. Gene Ther 2004;11:819–28.
25. Yoshida M, Kijima M, Akita M, Beppu T. Potent and specific inhibition of mammalian histone deacetylase both *in vivo* and *in vitro* by trichostatin A. J Biol Chem 1990;265:17174–9.
26. Lin X, Nelson WG. Methyl-CpG-binding domain protein-2 mediates transcriptional repression associated with hypermethylated GSTP1 CpG islands in MCF-7 breast cancer cells. Cancer Res 2003;63:498–504.
27. Richards EJ, Elgin SC. Epigenetic codes for heterochromatin formation and silencing: rounding up the usual suspects. Cell 2002;108:489–500.

28. Nan X, Ng HH, Johnson CA, et al. Transcriptional repression by the methyl-CpG-binding protein MeCP2 involves a histone deacetylase complex. Nature 1998;393: 386–9.
29. Dillon N, Festenstein R. Unravelling heterochromatin: competition between positive and negative factors regulates accessibility. Trends Genet 2002;18:252–8.
30. Zhang Y, Reinberg D. Transcription regulation by histone methylation: interplay between different covalent modifications of the core histone tails. Genes Dev 2001;15:2343–60.
31. Nguyen CT, Weisenberger DJ, Velicescu M, et al. Histone H3-lysine 9 methylation is associated with aberrant gene silencing in cancer cells and is rapidly reversed by 5-aza-2'-deoxycytidine. Cancer Res 2002;62: 6456–61.
32. McInerney JM, Nawrocki JR, Lowrey CH. Long-term silencing of retroviral vectors is resistant to reversal by trichostatin A and 5-azacytidine. Gene Ther 2000;7: 653–63.
33. Singer J, Stellwagen RH, Roberts-Ems J, Riggs AD. 5-Methylcytosine content of rat hepatoma DNA substituted with bromodeoxyuridine. J Biol Chem 1977;252: 5509–13.
34. Schwartz SA. Transcriptional activation of endogenous rat retrovirus with and without hypomethylation of proviral DNA. Biochem Biophys Res Commun 1983; 112:571–7.
35. Hutchins AS, Mullen AC, Lee HW, et al. Gene silencing quantitatively controls the function of a developmental *trans*-activator. Mol Cell 2002;10:81–91.
36. Lembo F, Pero R, Angrisano T, et al. MBDin, a novel MBD2-interacting protein, relieves MBD2 repression potential and reactivates transcription from methylated promoters. Mol Cell Biol 2003;23:1656–65.
37. Amedeo P, Habu Y, Afsar K, Scheid OM, Paszkowski J. Disruption of the plant gene MOM releases transcriptional silencing of methylated genes. Nature 2000;405: 203–6.
38. Fasy TM, Cullen BR, Luk D, Bick MD. Studies on the enhanced interaction of halodeoxyuridine-substituted DNAs with H1 histones and other polypeptides. J Biol Chem 1980;255:1380–7.
39. Graves BJ, Eisenman RN, McKnight SL. Delineation of transcriptional control signals within the Moloney murine sarcoma virus long terminal repeat. Mol Cell Biol 1985;5:1948–58.

−39−

Mutations Conferring Resistance to Human Immunodeficiency Virus Type 1 Fusion Inhibitors Are Restricted by gp41 and Rev-Responsive Element Functions

Daisuke Nameki,[1] Eiichi Kodama,[1]* Mieko Ikeuchi,[1] Naoto Mabuchi,[2] Akira Otaka,[3]
Hirokazu Tamamura,[3] Mutsuhito Ohno,[2] Nobutaka Fujii,[3] and Masao Matsuoka[1]

*Laboratory of Virus Immunology[1] and Laboratory of Biochemistry,[2] Institute for Virus Research, Graduate School of
Pharmaceutical Science,[3] Kyoto University, Kyoto, Japan*

One of the human immunodeficiency virus (HIV) envelope proteins, gp41, plays a key role in HIV fusion. A gp41-derived peptide, T-20, efficiently inhibits HIV fusion and is currently approved for treatment of HIV-infected individuals. Although resistant variants have been reported, the mechanism of the resistance remains to be defined. To elucidate the mechanism in detail, we generated variants resistant to C34, a peptide derived from the gp41 carboxyl terminus heptad repeat (C-HR) in vitro. The resistant variants had a 5-amino-acid deletion in gp120 and a total of seven amino acid substitutions in gp41. Binding assays revealed that an I37K substitution in the N-terminal heptad repeat (N-HR) impaired the binding of C34, whereas an N126K substitution in the C-HR enhanced the binding to mutated N-HR, indicating that both mutations were directly involved in resistance. On the other hand, substitutions for A30 and D36 seemed to be secondary mutations, located complementary to each other in the Rev-responsive element (RRE), and were mutated simultaneously to maintain the secondary structure of the RRE that was impaired by the mutations at I37. Thus, HIV acquired resistance to C34 by mutations in N-HR, which directly interacted with C34. However, since this region also encoded the RRE, additional mutations were required to maintain viral replication. These results suggest that HIV fusion is one of the attractive targets for HIV chemotherapy.

Peptide inhibitors that block human immunodeficiency virus type 1 (HIV-1) fusion were first reported by Wild et al. (30). Recently, a peptide fusion inhibitor (T-20 or enfuvirtide) has been approved in the United States and Europe for treatment of HIV-infected individuals. The peptide sequence of T-20 is derived from the gp41 C terminus heptad repeat (C-HR) sequence, which corresponds to a linear region of 36 amino acids, and T-20 inhibits fusion by binding to the N-terminal heptad repeat (N-HR) of gp41 and preventing 6-helix bundle formation (4, 30). In HIV-infected patients, the effect of T-20 in combination with an antiretroviral regimen that was optimized with the aid of phenotypic and genotypic resistance testing (TORO 1 and 2) has been reported to suppress drug-resistant HIV replication more efficiently that the optimized regimen alone (17, 18).

The emergence of T-20-resistant HIV-1 was first reported in clinical patients receiving T-20 monotherapy in a phase I clinical trial (28) and subsequently in combined regimens employed in phase II and III trials of T-20 (23, 25). The T-20 susceptibility of recombinant HIV-1 containing the identified substitutions was examined in vitro and considered to be moderately resistant (5.4- to 6.3-fold) (28). However, the detailed mechanism of resistance of these variants still remains to be elucidated. On the other hand, Rimsky et al. revealed that three continuous amino acids in the N-HR (GIV at positions 36 to 38 of gp41) were crucial for the inhibition of HIV-1 entry

by T-20 and for efficient association between N-HR and T-20 in vitro (26). Fikkert et al. also reported that HIV-1 variants resistant to T-20 contained substitutions in gp41, L33S and N43K, and a deletion of 5 amino acids, FNSTW (ΔFNSTW), in the V4 region of gp120 (9). L33S and N43K contributed to T-20 resistance, whereas the 5-amino-acid deletion alone had little effect on T-20 sensitivity. These results suggest that substitutions in the N-HR directly affect T-20 binding. Although the baseline sensitivity of HIV-1 to T-20 is defined by amino acid substitutions in gp41, coreceptor specificity is influenced by substitutions in the V3 loop in gp120, affects the fusion kinetics, and modulates T-20 sensitivity (4, 5).

To elucidate the mechanism of resistance to the peptide fusion inhibitors, we generated and characterized HIV-1 variants resistant to C34, a gp41 C-HR-derived peptide (2, 22) (Fig. 1A). During the selection of C34-resistant variants, we observed a 5-amino-acid deletion in the gp120 V4 region and a total of seven amino acid substitutions in gp41. Among the deletion and the substitutions, I37K and N126K play a key role in the resistance to C-HR-derived peptides, including T-20. Other deletions or substitutions were considered to enhance C34 resistance and/or improve the impaired replication kinetics. A30V and D36G maintained the Rev-responsive element (RRE) structure destabilized by I37T and I37K, respectively. Thus, these results reveal that the deletions or substitutions conferring resistance are restricted by both gp41 and RRE functions, suggesting that HIV-1 fusion is one of the most ideal targets for chemotherapy.

MATERIALS AND METHODS

Cells and viruses. MT-2 and Cos-7 cells were grown in RPMI 1640- and Dulbecco's modified Eagle medium-based culture medium, respectively. HeLa-

* Corresponding author. Mailing address: Laboratory of Virus Immunology, Institute for Virus Research, Kyoto University, 53 Shogoin Kawaramachi, Sakyoku, Kyoto 606-8507, Japan. Phone 81-75-751-3986. Fax: 81-75-751-3986. E-mail: ekodama@virus.kyoto-u.ac.jp.

A

RRE coding region   Extracellular   Intracellular

NH₂   FP   N-HR   C-HR   TM   //   COOH

36   N36   71   127   T-20   162

--LLSDIVQQQNNLLRAIEAQQHLLQLTVWGIKQLQARIL--

--LLSSIMQQQNN--
--LLSDTVQQQNN--   T-20ʳ
--SLSDIVQQQNK--

117   C34   150

--WMEWDREINNYTSLIHSLIEESQNQQEKNEQELLELDKWASLWNWF--   --YSPLSF--

----SGKVQQQNN--   C34ʳ   --INKYT--   --YSPISF--

B

EC₅₀ (μM)

| 0.002 | 0.004 | 0.016 | 0.2 | 0.58 |

Concentration of C34 (μM)

Q39H   N126K

A30V I371/T N126K

A30V I37T N126K

D36G I37K N126K L204I
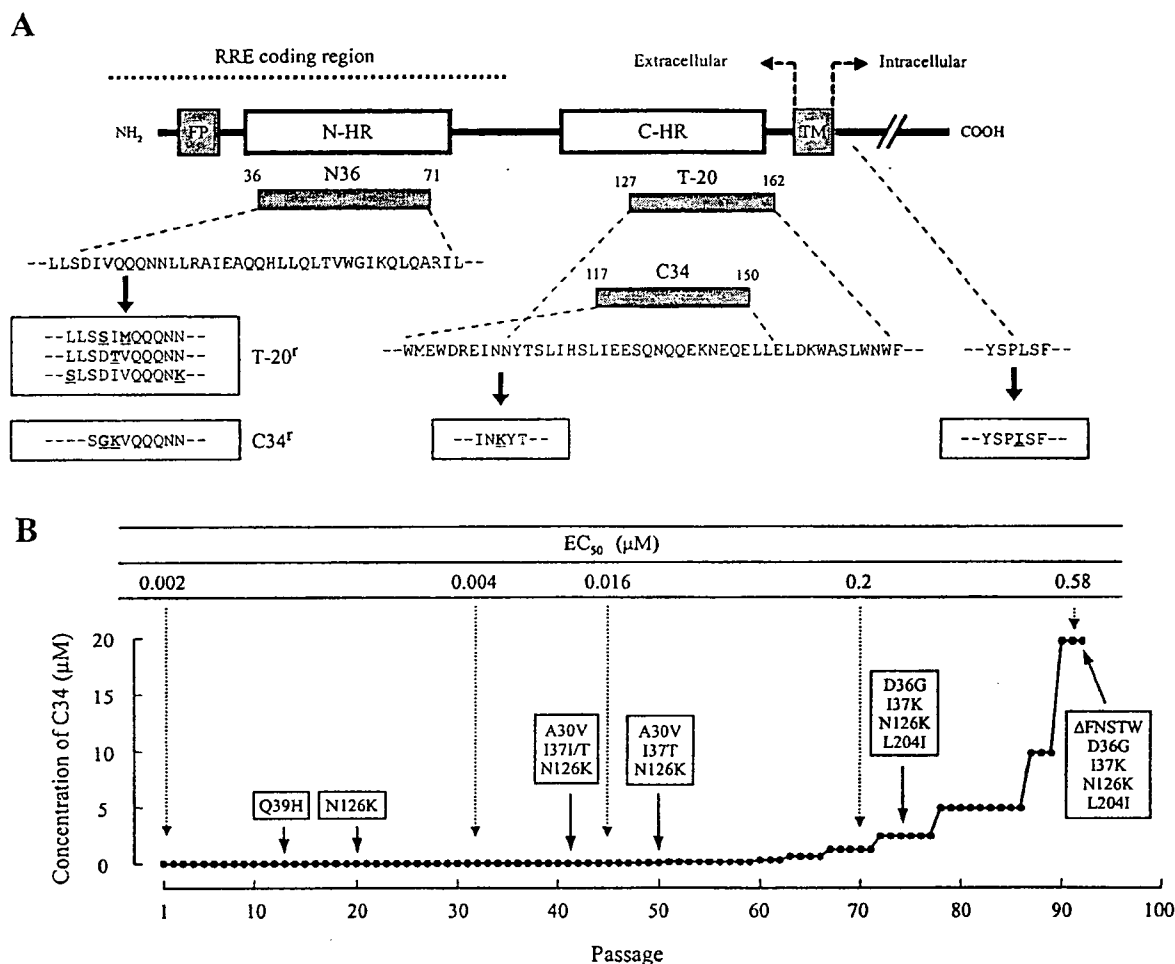
ΔFNSTW D36G I37K N126K L204I

Passage

FIG. 1. Schematic view of HIV-1 gp41 (A) and induction of C34-resistant HIV-1 (B). The locations of the fusion peptide (FP), N-terminal heptad repeat region (N-HR), C-terminal heptad repeat region (C-HR), transmembrane domain (TM), various gp41-derived peptides, and the Rev-responsive element (RRE) coding region are shown (A). The residue numbers of each peptide correspond to their positions in gp41. The bold underlined letters in the boxes indicate the novel mutations that have been reported in T-20-resistant HIV-1 variants (T-20ʳ) in vitro (9, 26) and that have been observed in C34-resistant HIV-1 variants (C34ʳ). (B) HIV-1$_{NL4-3}$ was passaged in the presence of increasing concentrations of C34 in MT-2 cells. The dose-escalating selection was carried out for a total of 93 passages, with compound concentrations ranging from 0.0001 to 20 μM. At the indicated passages, proviral DNAs from the lysates of infected cells were sequenced, and the EC₅₀s of the HIV-1 variants were determined with the MAGI assay.

CD4-LTR-β-gal cells were kindly provided by M. Emerman through the AIDS Research and Reference Reagent Program, Division of AIDS, National Institute of Allergy and Infectious Disease (Bethesda, Md.), and used for the drug susceptibility assay (multinuclear activation of galactosidase indicator [MAGI] assay) as described previously (12, 14, 21). An HIV-1 infectious clone, pNL4-3, which was kindly provided by H. Sakai, Institute for Virus Research, Kyoto University (Kyoto, Japan), was used for constructions and the production of HIV-1 variants. A wild-type HIV-1, HIV-1$_{WT}$, was generated by transfection of pNL4-3 into Cos-7 cells.

Antiviral agents. The peptides used were N36, derived from the N-HR of gp41, and C34 and T-20, derived from the C-HR of gp41. The peptides were synthesized as described previously (24) and are depicted in Fig. 1A. 2′,3′-Dideoxycytidine (ddC) was purchased from Sigma (St. Louis, Mo.).

Determination of drug susceptibility of HIV-1. The peptide sensitivity of infectious clones was determined by the MAGI assay with some modifications (14, 21). Briefly, the target cells (HeLa-CD4-LTR-β-gal; 10⁴ cells/well) were plated in 96-well flat microtiter culture plates. On the following day, the cells were inoculated with the HIV-1 clones (60 MAGI U/well, giving 60 blue cells after 48 h of incubation) and cultured in the presence of various concentrations of drugs in fresh medium. Forty-eight hours after viral exposure, all the blue cells

stained with X-Gal (5-bromo-4-chloro-3-indolyl-β-D-galactopyranoside) were counted in each well. The activity of test compounds was determined as the concentration that blocked HIV-1 replication by 50% (50% effective concentration [EC₅₀]).

Construction of recombinant HIV-1 clones. Recombinant infectious HIV-1 clones carrying various mutations in gp120 and/or gp41 were generated by using pNL4-3. Briefly, the desired mutations were introduced into the NheI-BamHI region (1,220 bp) of pSL-gp41$_{WT}$, which encoded nucleotides 7250 to 8469 of pNL4-3, by an oligonucleotide-based mutagenesis method (29). NheI-BamHI fragments were inserted into pNL4-3, generating various molecular clones with the desired mutations. Each molecular clone was transfected into Cos-7 cells (10⁵ cells/six-well culture plate). After 48 h, MT-2 cells (10⁶ cells/well) were added and cocultured with the Cos-7 cells for an additional 24 h. When an extensive cytopathic effect (CPE) was observed, the supernatants were harvested and stored at −80°C until use.

Generation of HIV-1 variants resistant to C34. MT-2 cells were exposed to HIV-1$_{WT}$ and cultured in the presence of C34 at an initial concentration of 0.0001 μM. Cultures were incubated at 37°C until an extensive CPE was observed. The culture supernatants were used for further passages in MT-2 cells in the presence of twofold increasing concentrations of C34 when massive CPEs

were seen in the earlier periods. Such dose-escalating culture was performed until resistant variants were obtained. This selection was carried out for a total of 93 passages. At the indicated passages (Fig. 1B), the sequence of the *env* region was determined by direct sequencing of the proviral DNA extracted from the infected MT-2 cells.

Viral replication kinetics assay. MT-2 cells (10^5 cells/5 ml) were infected with each virus preparation (500 MAGI U) for 4 h. The infected cells were then washed and cultured in a final volume of 5 ml. The culture supernatants (100 μl) were harvested on days 1, 2, 4, 6, and 8 after infection, and the p24 antigen amounts were determined.

For competitive HIV-1 replication assays (CHRA), two titrated infectious clones to be examined were mixed and added to MT-2 cells (10^5 cells/3 ml) as described previously (15) with some modifications. To ensure that the two infectious clones being compared were of approximately equal infectivity, a fixed amount (500 MAGI U) of one infectious clone was mixed with three different amounts (250, 500, and 1,000 MAGI U) of the other infectious clone. On day 1, one third of the infected MT-2 cells were harvested and washed twice with phosphate-buffered saline, and the cellular DNA was extracted. The purified DNA was subjected to nested PCR and then direct DNA sequencing. The HIV-1 coculture which best approximated a 50:50 mixture on day 1 was further propagated. Every 6 to 7 days, the cell-free supernatant of the virus coculture (1 ml) was transmitted to new uninfected MT-2 cells. The cells harvested at the end of each passage were subjected to direct sequencing, and the viral population change was determined.

Binding assay. Each peptide (40 μM) was mixed with 10 mM phosphate-buffered saline–140 mM NaCl, pH 7.4, in an Aviv model 202 DS spectrometer equipped with a thermoelectric temperature controller. The thermal stability was assessed by monitoring the change in the circular dichroism signal at 222 nm. The midpoint of the thermal unfolding transition (melting temperature [T_m]) of each complex was determined as described previously (24).

Gel shift assay. RNA of the RRE region and recombinant Rev were prepared as described previously (10) with some modifications. Briefly, the RRE region of the variants (nucleotides 7748 to 8009 of pNL4-3) was introduced into pBlue-Script (Stratagene, La Jolla, Calif.). In vitro RNA transcription was performed with T7 RNA polymerase and [^{32}P]UTP. Recombinant Rev was generated by use of the pGEX-6P-1/BL21 expression system (Amersham Biosciences, Piscataway, N.J.). The RNA and Rev were mixed at 25°C for 20 min in binding buffer (50 mM Tris-HCl, pH 7.5, 150 mM KCl, 1 mM dithiothreitol, 8% glycerol, 50 μg of tRNA/ml, and 100 μg of bovine serum albumin/ml) and subjected to native acrylamide gel electrophoresis.

RESULTS

Amino acid substitutions identified in the *env* region of C34-resistant HIV-1. At passage 14 (P-14) in the culture where HIV-1 was propagating in the presence of C34 (0.0032 μM), one amino acid substitution, glutamine to histidine at position 39 (Q39H), in the N-HR of gp41 was transiently identified (Fig. 1B). At P-20 (0.0064 μM), a substitution, N126K, was newly identified in the C-HR, whereas Q39H had returned to the original wild-type amino acid. At P-41 (0.026 μM), two substitutions, A30V and I37I/T (mixture of I and T), were observed in the N-HR in addition to N126K, while at P-50 (0.077 μM), definitive I37T was detected (A30V/I37T/N126K) (Fig. 1B). At P-75 (2.5 μM), A30V had returned to the original wild-type amino acid, D36G was detected, I37T was substituted for I37K, and L204I, which was located in the cytoplasmic domain of gp41, was identified (D36G/I37K/N126K/ L204I). At P-92 (20 μM), a deletion of five amino acids, FNSTW, in the V4 loop of gp120 (ΔFNSTW) was observed together with the four substitutions (ΔFNSTW/D36G/I37K/ N126K/L204I) (Fig. 1B). In addition to the *env* region, we also examined the Tat- and Rev-encoding regions but did not observe any substitutions. These results suggest that, in order to develop a higher resistance to C34, HIV-1 acquires not only multiple substitutions in gp41 but also the 5-amino-acid deletion in gp120.

Susceptibility of the different *env* recombinant viruses to fusion inhibitors. To clarify which substitutions among the identified changes were responsible for C34 resistance, we first generated infectious HIV-1 clones containing the deletion (ΔFNSTW) in gp120 or the single amino acid substitutions (A30V, D36G, I37T, I37K, Q39H, N126K, or L204I) in gp41 that were observed during the selection procedure (Fig. 1B). We also evaluated the activities of the gp41-derived peptides N36, T-20, and C34 and a reverse transcriptase inhibitor used as a control, ddC, against these strains with the MAGI assay (Table 1).

HIV-1$_{\Delta FNSTW}$, HIV-1$_{A30V}$, HIV-1$_{Q39H}$, and HIV-1$_{L204I}$ showed weak resistance to C34 compared with HIV-1$_{WT}$ (less than fivefold). Interestingly, D36G, observed in the majority of HIV-1 strains (16), conferred an increased T-20 susceptibility to HIV-1 (10-fold), in agreement with previous reports (20, 26), whereas D36G did not contribute C34 resistance by itself (0.8-fold). Although I37T has also been reported as one of the T-20 resistance mutations in vitro, its detailed mechanism of resistance remains unknown (20, 26). In our experiments, I37T conferred T-20 and C34 resistance to HIV-1 (13- and 11-fold, respectively), and I38K also conferred both T-20 and C34 resistance (212- and 13-fold, respectively). HIV-1$_{N126K}$ showed moderate resistance to C34 (6.8-fold). Neither the deletion in gp120 nor any of the substitutions in gp41 conferred resistance to N36 or ddC (Table 1).

Although the I37 substitutions appeared to be primarily responsible for C34 resistance, the C34 resistance levels of the I37 substitution variants were not comparable to that of the selected virus at P-93 (EC$_{50}$, 0.78 μM). Therefore, we generated infectious HIV-1 clones containing the identified substitutions combined with I37T or I37K and determined their susceptibilities to the peptides (Table 1). The combination of I37K and N126K enhanced C34 resistance (13- to 28-fold), whereas HIV-1$_{I37T}$, HIV-1$_{I37T/N126K}$, and HIV-1$_{A30V/I37T/N126K}$ showed comparable resistance levels to C34. Moreover, I37K/N126K combined with D36G (D36G/I37K/N126K) enhanced C34 resistance (72-fold), although the L204I substitution combined with D36G/I37K/N126K decreased the levels of resistance to both T-20 and C34 (10- and 54-fold, respectively). A clone containing the deletion in gp120 and four substitutions in gp41, HIV-1$_{\Delta FNSTW/D36G/I37K/N126K/L204I}$, showed the highest resistance to C34 (83-fold) and cross-resistance to T-20 (64-fold). These results indicate that the I37K substitution is mainly responsible for C34 resistance, whereas the other substitutions enhance the resistance or improve the impaired viral replication kinetics.

Next, we generated a T-20-resistant molecular clone which had been previously reported (26), HIV-1$_{D36S/V38M}$, and evaluated the susceptibility to N36, T-20, and C34. HIV-1$_{D36S/V38M}$ showed moderate resistance to both T-20 and C34 (5.1- and 7.7-fold, respectively) (Table 1). We also generated HIV-1 variants that contained each of the single substitutions, HIV-1$_{D36S}$ and HIV-1$_{V38M}$. HIV-1$_{D36S}$ did not contribute to the resistance, although HIV-1$_{V38M}$ showed cross-resistance to T-20 and C34 (26- and 15-fold, respectively). Combined with the finding that I37K is the major mutation for resistance to C34, this region, positions 37 and 38 of gp41, appears to be involved in resistance to both T-20 and C34, while changes at position 36 appear to be largely restricted in their effects to T-20.

TABLE 1. Antiviral activity of HIV-1 gp41-derived peptides against gp120 and/or gp41 recombinant viruses[a]

Virus or substitution	EC$_{50}$ (nM)			
	ddC	T-20	N36	C34
HIV-1$_{WT}$[b]	264	12	51	2.1
ΔFNSTW[c]	98 (0.4)	18 (1.5)	50 (1.0)	9.5 (4.6)
A30V	205 (0.8)	6.3 (0.5)	38 (0.7)	7.0 (3.4)
D36G	173 (0.7)	0.92 (0.1)	90 (1.7)	1.6 (0.8)
D36S[c]	166 (0.6)	6.6 (0.6)	89 (1.7)	3.7 (0.6)
I37T	284 (1.1)	156 (13)	40 (0.8)	23 (11)
I37K	326 (1.2)	2,482 (212)	99 (1.9)	27 (13)
V38M[c]	223 (0.8)	305 (26)	94 (1.8)	31 (15)
Q39H[d]	330 (1.3)	1.9 (0.2)	165 (3.2)	5.3 (2.6)
N126K[d]	380 (1.4)	23 (1.9)	137 (2.7)	14 (6.8)
L204I	247 (0.9)	13 (1.1)	105 (2.0)	4.4 (2.1)
D36S/V38M[c]	294 (1.1)	60 (5.1)	46 (0.9)	16 (7.7)
I37T/N126K	292 (1.1)	158 (14)	54 (1.1)	22 (11)
I37K/N126K	309 (1.2)	1,570 (134)	51 (1.0)	57 (28)
A30V/I37K/N126K	409 (1.5)	198 (17)	119 (2.3)	22 (10)
D36G/I37K/N126K	329 (1.2)	269 (23)	156 (3.0)	148 (72)
D36G/I37K/N126K/L204I[d]	209 (0.8)	117 (10)	41 (1.2)	112 (54)
ΔFNSTW/D36G/I37K/N126K/L204I[d]	213 (0.8)	746 (64)	54 (1.0)	171 (83)

[a] Anti-HIV activity was determined with the MAGI assay. The data shown are mean values obtained from the results of at least three independent experiments, and resistance (n-fold) in EC$_{50}$ for recombinant viruses compared to HIV-1$_{WT}$ is shown in parentheses.
[b] HIV-1$_{NL4-3}$ was used was a wild-type virus.
[c] ΔFNSTW is the deletion of 5 amino acids at positions 364 to 368 in the gp120 V4 region of HIV-1$_{NL4-3}$.
[d] Mutant viruses observed during induction of C34 resistance variants in vitro (Fig. 1B).
[e] D36S/V38M has been reported for T-20-resistant HIV-1 variants (26).

Peptide binding affinity. To clarify the effect of the substitutions on the interaction of N-HR and C-HR, the binding affinity of the peptides in vitro was examined with the synthesized peptides (Table 2). The affinity between N36$_{D36G/I37K}$ and C34 was unstable even at 37°C, indicating that the peptide inhibitor C34 hardly bound to N36$_{D36G/I37K}$. However, it is still unclear whether it is a direct effect of the N-HR mutations decreasing the affinity of C34 binding or an indirect effect of the N-HR mutations destabilizing the N-HR trimer formation. In contrast, C34$_{N126K}$, with the substitution responsible for the resistance, showed enhanced binding affinity not only to N36 but also to N36$_{D36G/I37K}$. Thus, there are two implications of mutations in gp41 for conferring C34 resistance: the decreased affinity of C34 for N36$_{D36G/I37K}$ and the increased affinity of C34$_{N126K}$ for both N36$_{WT}$ and N36$_{D36G/I37K}$. In other words, the D36G and I37K substitutions in the N-HR interfere with the binding of the peptide inhibitors, such as T-20 and C34, and N126K in the C-HR enhances the intra-gp41 binding of N-HR and C-HR compared with the peptide inhibitors.

Replication kinetics of C34-resistant variants. To determine the effects of the identified deletion and mutations on HIV-1 replication, we first examined the replication kinetics of HIV-1 variants by p24 production in the culture supernatants. The p24 production by the variants ranged from 14 to 34% of that

TABLE 2. Binding affinity of wild and mutated peptides[a]

Peptide	T_m (°C)
N36/C34	49.5
N36$_{D36G/I37K}$/C34	38.5
N36/C34$_{N126K}$	55.0
N36$_{D36G/I37K}$/C34$_{N126K}$	45.0

[a] The binding affinity of the peptides is shown with T_m values.

of HIV-1$_{WT}$ (HIV-1$_{I37T/N126K}$, 14%; HIV-1$_{N126K}$, 30%; and HIV-1$_{A30V/I37T/N126K}$, 34%) as determined at day 8 (Fig. 2). Next, the replication levels of variants with representative substitutions were compared by CHRA. The resistances (n-fold) of the variants are also shown in Fig. 2. Since HIV-1$_{Q39H}$ was considered to be one of the polymorphisms and appeared only transiently, we first compared the replication of HIV-1$_{WT}$ and HIV-1$_{N126K}$ and found an impaired replication profile for HIV-1$_{N126K}$. The variant with a combination including the I37T substitution, HIV-1$_{I37T/N126K}$, which was not observed during selection, showed the slowest replication profile. To develop an HIV-1$_{A30V/I37T/N126K}$ variant, the A30V substitution was introduced first, and then the I37T substitution was introduced (Fig. 1B). This was consistent with the results of the CHRA that the replication profile of HIV-1$_{A30V/I37T/N126K}$ was
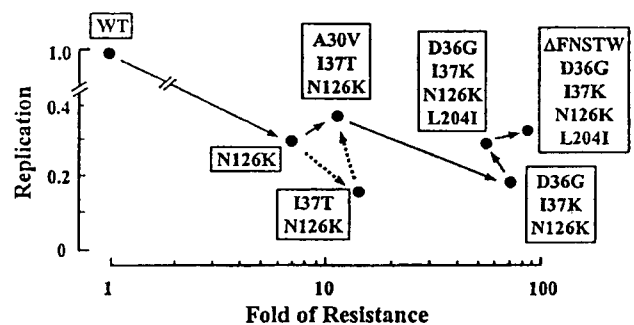

FIG. 2. Replication kinetics of the resistant variants. The replication kinetics determined by p24 antigen production and the CHRA are summarized. The data are depicted as the resistance (x axis) and replication (y axis) compared with those of HIV-1$_{WT}$. Variants observed (continuous arrows) and not observed (dashed arrows) in the selection are shown in the order of their emergence.
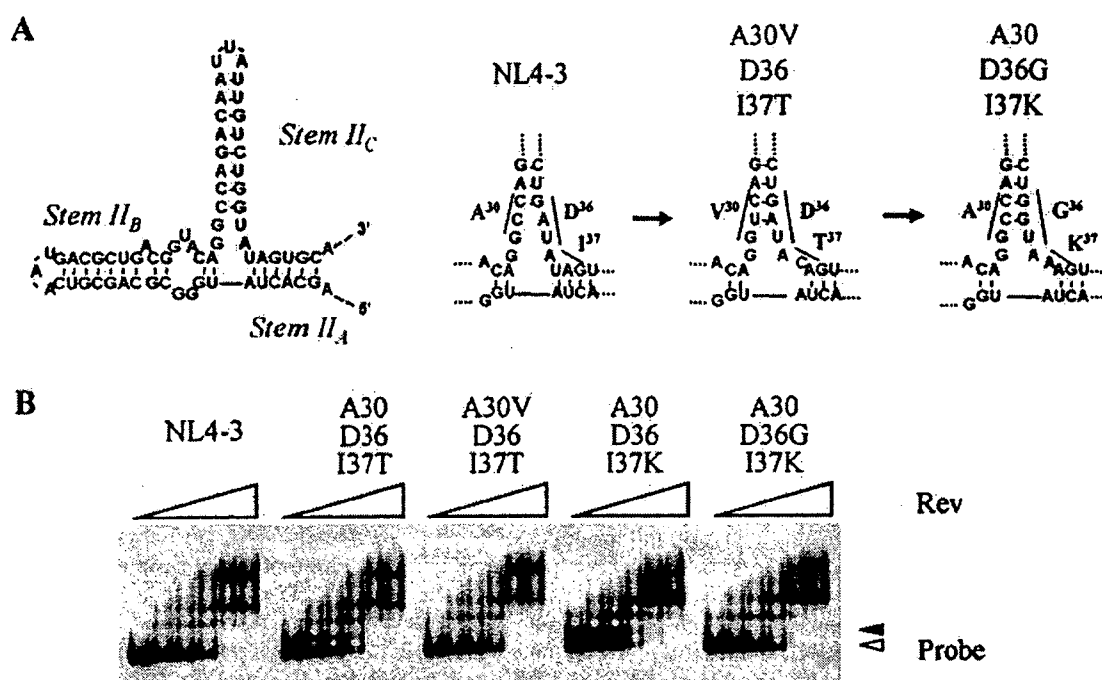
FIG. 3. Putative secondary structure of the RRE and locations of the nucleotides corresponding to the substitutions. The II_A, II_B, and II_C stems and the effects of the nucleotide substitutions are shown (A). A30V (GCC to G<u>T</u>C) to D36 (<u>GA</u>T) and A30 (G<u>CC</u>) to D36G (GAT to <u>GG</u>T) are located complementary to each other in the stem II_B (underlined). The effects of the nucleotide substitutions on the Rev-RRE interaction were examined by gel shift assays (B). The RRE of HIV-1$_{I37T}$ and HIV-1$_{I37K}$ displayed two signals. The amounts of Rev used were 0, 20, 40, 80, 160, 240, and 320 nM (left to right).

greater than that of HIV-1$_{I37T/N126K}$, suggesting that the A30V substitution improved the impaired replication profile of HIV-1$_{I37T/N126K}$. Since both HIV-1$_{I37K}$ and HIV-1$_{I37K/N126K}$ could replicate for only a few passages, these variants could not be studied. For I37K/N126K substitutions, D36G instead of A30V substitution seemed to be suitable in order to maintain resistance and replication, although the replication of HIV-1$_{D36G/I37K/N126K}$ still remained impaired. The L204I substitution improved the replication kinetics of HIV-1$_{D36G/I37K/N126K}$. The deletion in the V4 region contributed to both the increased resistance and replication. These results indicate that among the deletion and the substitutions, I37T/K and N126K, and especially I37K, are related to resistance, while A30V, D36G, and L204I are associated with improvement of replication and the deletion in the V4 region had modest effects on increased resistance and replication.

Rev and RRE interactions. The nucleotides for the substitutions A30V, D36G, and I38T/K also encode the RRE, and the nucleotides for A30 and D36 are located complementary to each other in stem II_C (Fig. 3A). A30V emerged along with I37T and intact D36, and D36G was found with I37K and intact A30. Thus, these mutations were thought to maintain the positioning of stems II_A and II_B in the tertiary structure of the RRE. To examine the effect of these nucleotide substitutions on the Rev-RRE interaction, we performed a gel shift assay. The secondary structure of the RRE that contained the I37T or I37K substitutions showed two forms (Fig. 3B). Introduction of A30V, which could improve the replication of HIV-1$_{I37T}$, changed the two RRE structures into a structure identical to that observed in the wild type. D36G observed with

I37K also changed the separated RRE structure. However, little difference (less than 10%) in the Rev binding caused by the substitutions was observed between the wild-type and the mutated RRE (Fig. 3B). These results indicate that substitutions at A30 or D36 maintain the stability of the RRE secondary structure that is affected by nucleotide substitutions at I37.

DISCUSSION

After adsorption to cells followed by conformational changes of gp120, HIV fusion takes place by interaction and binding of the N-HR and C-HR of gp41. C-HR-derived peptides, e.g., T-20 or C34, inhibit HIV replication as a decoy for C-HR (2, 30). Previous reports showed that mutations in N-HR (19) were associated with resistance to T-20 (9, 25, 26, 28). In this study, we showed that competition between C34 and C-HR also plays a key role in acquiring resistance. However, in order to develop high resistance to C34, changes in the binding affinity of N-HR, as observed in T-20 resistance, are insufficient on their own, and an additional mutation in C-HR is necessary. According to the crystal structure of gp41 (2), none of the substitutions observed in this study are located on the binding surface of the N-HR or C-HR. Even one of the primary mutations that directly contribute to the resistance, I37K, is not located on the binding surface of N-HR. We also identified a primary mutation, N126K, that is located outside of the binding surface of C-HR. Although the significance of these locations still remains to be defined at present, further structural analysis may provide insights into the mechanism of binding

enhancement. Our observations also provide evidence that small compounds interacting directly with the binding surface seem to inhibit HIV replication efficiently, since HIV would hardly be mutated on the binding surface.

During the selection of the C34-resistant variants, the substitutions were introduced in the following order: a substitution (N126K) associated with susceptibility to C34 was introduced first, followed by a substitution (A30V) associated with replication. L204I also improved the replication kinetics of HIV-$1_{D36G/I37K/N126K}$. It is likely that substitutions that are associated with resistance usually impair the replication kinetics, resulting in selection of HIV-1 variants containing substitutions that improve the replication disadvantages. This hypothesis has been proved with analyses of replication kinetics of T-20-resistant variants described previously (20). Moreover, such substitution patterns have previously been observed in multi-dideoxynucleoside-resistant variants (15, 21). However, the mechanism of replication improvement in multi-dideoxynucleoside-resistant variants remains unknown. In this study, I37 is one of the key amino acids for C34 resistance, and it is located in an important region for the Rev-RRE interaction (13). The significance of the secondary mutations, A30V and D36G, for improvement of the RRE structural stability impaired by I37T or I37K is thought to be that they maintain both gp41 and RRE functions. In contrast to the C34 resistance mutations, nucleotides encoding some T-20 resistance mutations, L33S and N43K (9), are located in a single-stranded bulge region of the stem II_C loop top (UUA to UCA) (Fig. 3A) and in the bulge region of stem III, indicating that the structural changes to the RRE would be minimal, while other T-20 resistance mutations (20), such as G36D, G36S, I37K, and possibly V38A and V38 M, appear to alter the stability of the RRE stem II_C structure and to impair the replication kinetics. To date, the Rev-RRE interaction has mainly been examined for stem II_B, since Rev directly binds to it (10, 13). Although the functions of stems II_A and II_C remain to be defined, it is possible that the secondary mutations in stem II_C influence the Rev-RRE interaction, since we have shown that the secondary mutations were introduced simultaneously with the primary mutations and improved replication. These results also indicate that the conformation of the RRE is essential for the Rev-RRE interaction and not just the nucleotide sequence of the RRE itself.

NL4-3 gp41 contains four N-glycan attachment sites, N-X-S/T, located at N100-A-S, N105-K-S, N114-M-T, and N126-Y-T. These four sites are highly conserved in various HIV strains (11, 16). Mutational analysis revealed that each substitution of the N glycosylation sites had a modest effect on HIV replication, whereas some combined substitutions severely impaired replication (11). Although the effect of N126-glycan on binding of the N-HR and C-HR remains unknown, it would be possible that N126-glycan plays some roles for C34 resistance. Different effects of N126K substitution on susceptibility to T-20 and C34 (1.9- and 6.8-fold, respectively) were observed (Table 1). This result might be accounted for by the finding that N126 locates at −1 (outside) from the N terminus of T-20, whereas it locates inside (+10) of C34 (Fig. 1A).

It has been reported that a tyrosine-based sorting signal in the gp41 cytoplasmic domain, Y201-X-X-L, was involved in trafficking and targeting to the plasma membrane of the gp41

(3). The motif is highly conserved among various HIV strains (16, 19). Although the role of Y201 for infectivity has been studied in detail (3, 19), that of L204 remains to be defined. In the present study, we showed that the L204I substitution enhanced viral replication, suggesting that L204, as well as Y201, plays an important role for viral replication.

pNL4-3 was established as a molecular clone of wild-type HIV-1 (1) and is widely used in HIV research. However, it represents only one of the wild-type HIV-1 variants. In fact, even in the absence of C34, we still observed several substitutions in NL4-3 that were identified in the C34 selection, e.g., A30V and Q39H. These substitutions are also observed in some treatment-naïve clinical isolates (16). It is well known that HIV reverse transcriptase makes several nucleotides miss incorporation during the reverse transcription, suggesting that each HIV isolate, even in the wild-type population, contains several substitutions in the integrated DNA genome. D36 is identified only in pNL4-3-derived clones, although the G36/I37/V38 motif is well conserved, not only in HIV-1 but also in HIV-2 and simian immunodeficiency virus strains (16). Furthermore, the 5-amino-acid deletion in gp120 was reported not only in a fusion inhibitor, T-20 (9), but also in CD4-gp120-binding inhibitors DS5000 (8) and AR177 (Zintevir) (7), CXCR4 antagonists, bicyclams JM2763 and SID791 (6), and SDF-1α-resistant variants (27). In these reports, pNL4-3-derived viruses were also used for the selection of the resistant variants. Only pNL4-3 has the 5-amino-acid tandem sequence FNSTWFNSTW in the gp120 V4 region. Therefore, this deletion is thought to be specific for HIV-1_{NL4-3}, although the 5-amino-acid deletion conferred weak C34 resistance. These results indicate that we should be careful before concluding that such substitutions are involved in the resistance or replication kinetics.

In conclusion, HIV acquires resistance against C34 by mutations in both N-HR and C-HR. However, mutations in N-HR are restricted by Rev-RRE and/or gp120-gp41 interactions, suggesting that HIV-1 fusion is one of the most attractive targets for blocking HIV infection.

REFERENCES

1. Adachi, A., H. E. Gendelman, S. Koenig, T. Folks, R. Willey, A. Rabson, and M. A. Martin. 1986. Production of the acquired immunodeficiency syndrome-associated retrovirus in human and nonhuman cells transfected with an infectious molecular clone. J. Virol. 59:284–291.
2. Chan, D. C., D. Fass, J. M. Berger, and P. S. Kim. 1997. Core structure of gp41 from the HIV envelope glycoprotein. Cell 89:263–273.
3. Day, J. R., C. Munk, and J. C. Guatelli. 2004. The membrane-proximal tyosine-based sorting signal of human immunodeficiency virus type 1 gp41 is required for optimal viral infectivity. J. Virol. 78:1069–1079.
4. Derdeyn, C. A., J. M. Decker, J. N. Sfakianos, X. Wu, W. A. O'Brien, L. Ratner, J. C. Kappes, G. M. Shaw, and E. Hunter. 2000. Sensitivity of human immunodeficiency virus type 1 to the fusion inhibitor T-20 is modulated by coreceptor specificity defined by the V3 loop of gp120. J. Virol. 74:8358–8367.

5. Derdeyn, C. A., J. M. Decker, J. N. Sfakianos, Z. Zhang, W. A. O'Brien, L. Ratner, G. M. Shaw, and E. Hunter. 2001. Sensitivity of human immunodeficiency virus type 1 to fusion inhibitors targeted to the gp41 first heptad repeat involves distinct regions of gp41 and is consistently modulated by gp120 interactions with the coreceptor. J. Virol. 75:8605–8614.

6. De Vreese, K., V. Kofler-Mongold, C. Leutgeb, V. Weber, K. Vermeire, S. Schacht, J. Anne, E. De Clercq, R. Datema, and G. Werner. 1996. The molecular target of bicyclams, potent inhibitors of human immunodeficiency virus replication. J. Virol. 70:689–696.

7. Este, J. A., C. Cabrera, D. Schols, P. Cherepanov, A. Gutierrez, M. Witvrouw, C. Pannecouque, Z. Debyser, R. F. Rando, B. Clotet, J. Desmyter, and E. De Clercq. 1998. Human immunodeficiency virus glycoprotein gp120 as the primary target for the antiviral action of AR177 (Zintevir). Mol. Pharmacol. 53:340–345.

8. Este, J. A., D. Schols, K. De Vreese, K. Van Laethem, A. M. Vandamme, J. Desmyter, and E. De Clercq. 1997. Development of resistance of human immunodeficiency virus type 1 to dextran sulfate associated with the emergence of specific mutations in the envelope gp120 glycoprotein. Mol. Pharmacol. 52:98–104.

9. Fikkert, V., P. Cherepanov, K. Van Laethem, A. Hantson, B. Van Remoortel, C. Pannecouque, E. De Clercq, Z. Debyser, A.-M. Vandamme, and M. Witvrouw. 2002. env chimeric virus technology for evaluating human immunodeficiency virus susceptibility to entry inhibitors. Antimicrob. Agents Chemother. 46:3954–3962.

10. Henderson, B. R. 1997. Interaction between HIV Rev and nuclear import and export factors: the Rev nuclear localisation signal mediates specific binding to human importin-β. J. Mol. Biol. 274:693–707.

11. Johnson, W. E., J. M. Sauvron, and R. C. Desrosiers. 2001. Conserved, N-linked carbohydrates of human immunodeficiency virus type 1 gp41 are largely dispensable for viral replication. J. Virol. 75:11426–11436.

12. Kimpton, J., and M. Emerman. 1992. Detection of replication-competent and pseudotyped human immunodeficiency virus with a sensitive cell line on the basis of activation of an integrated β-galactosidase gene. J. Virol. 66:2232–2239.

13. Kjems, J., M. Brown, D. D. Chang, and P. A. Sharp. 1991. Structural analysis of the interaction between the human immunodeficiency virus Rev protein and the Rev response element. Proc. Natl. Acad. Sci. USA 88:683–687.

14. Kodama, E. I., S. Kohgo, K. Kitano, H. Machida, H. Gatanaga, S. Shigeta, M. Matsuoka, H. Ohrui, and H. Mitsuya. 2001. 4'-Ethynyl nucleoside analogs: potent inhibitors of multidrug-resistant human immunodeficiency virus variants in vitro. Antimicrob. Agents Chemother. 45:1539–1546.

15. Kosalaraksa, P., M. F. Kavlick, V. Maroun, R. Le, and H. Mitsuya. 1999. Comparative fitness of multi-dideoxynucleoside-resistant human immunodeficiency virus type 1 (HIV-1) in an in vitro competitive HIV-1 replication assay. J. Virol. 73:5356–5363.

16. Kuiken, C., B. Foley, B. Hahn, P. Marx, F. McCutchan, J. Mellors, S. Wolinsky, and B. Korber (ed.). 2001. HIV sequence compendium 2001. Theoretical Biology and Biophysics Group, Los Alamos National Laboratory, Los Alamos, N.M.

17. Lalezari, J. P., K. Henry, M. O'Hearn, J. S. Montaner, P. J. Piliero, B. Trottier, S. Walmsley, C. Cohen, D. R. Kuritzkes, J. J. Eron, Jr., J. Chung, R. DeMasi, L. Donatacci, C. Drobnes, J. Delehanty, and M. Salgo. 2003.

18. Enfuvirtide, an HIV-1 fusion inhibitor, for drug-resistant HIV infection in North and South America. N. Engl. J. Med. 348:2175–2185.

18. Lazzarin, A., B. Clotet, D. Cooper, J. Reynes, K. Arasteh, M. Nelson, C. Katlama, H. J. Stellbrink, J. F. Delfraissy, J. Lange, L. Huson, R. DeMasi, C. Wat, J. Delehanty, C. Drobnes, and M. Salgo. 2003. Efficacy of enfuvirtide in patients infected with drug-resistant HIV-1 in Europe and Australia. N. Engl. J. Med. 348:2186–2195.

19. Lodge, R., J.-P. Lalonde, G. Lemay, and E. A. Cohen, 1997. The membrane-proximal intracytoplasmic tyrosine residue of HIV-1 envelope glycoprotein is critical for basolateral targeting of viral budding in MDCK cells. EMBO J. 16:695–705.

20. Lu, J., P. Sista, F. Giguel, M. Greenberg, and D. Kuritzkes. 2004. Relative replicative fitness of human immunodeficiency virus type 1 mutants resistant to enfuvirtide (T-20). J. Virol. 78:4628–4637.

21. Maeda, Y., D. J. Venzon, and H. Mitsuya. 1998. Altered drug sensitivity, fitness, and evolution of human immunodeficiency virus type 1 with pol gene mutations conferring multi-dideoxynucleoside resistance. J. Infect. Dis. 177:1207–1213.

22. Malashkevich, V. N., D. C. Chan, C. T. Chutkowski, and P. S. Kim. 1998. Crystal structure of the simian immunodeficiency virus (SIV) gp41 core: conserved helical interactions underlie the broad inhibitory activity of gp41 peptides. Proc. Natl. Acad. Sci. USA 95:9134–9139.

23. Matthews, T., M. Salgo, M. Greenberg, J. Chung, R. DeMasi, and D. Bolognesi. 2004. Enfuvirtide: the first therapy to inhibit the entry of HIV-1 into host CD4 lymphocytes. Nat. Rev. Drug Discov. 3:215–225.

24. Otaka, A., M. Nakamura, D. Nameki, E. Kodama, S. Uchiyama, S. Nakamura, H. Nakano, H. Tamamura, Y. Kobayashi, M. Matsuoka, and N. Fujii. 2002. Remodeling of gp41-C34 peptide leads to highly effective inhibitors of the fusion of HIV-1 with target cells. Angew. Chem. Int. Ed. Engl. 41:2937–2940.

25. Poveda, E., B. Rodes, C. Toro, L. Martin-Carbonero, J. Gonzalez-Lahoz, and V. Soriano. 2002. Evolution of the gp41 env region in HIV-infected patients receiving T-20, a fusion inhibitor. AIDS 16:1959–1961.

26. Rimsky, L. T., D. C. Shugars, and T. J. Matthews. 1998. Determinants of human immunodeficiency virus type 1 resistance to gp41-derived inhibitory peptides. J. Virol. 72:986–993.

27. Schols, D., J. A. Este, C. Cabrera, and E. De Clercq. 1998. T-cell-line-tropic human immunodeficiency virus type 1 that is made resistant to stromal cell-derived factor 1α contains mutations in the envelope gp120 but does not show a switch in coreceptor use. J. Virol. 72:4032–4037.

28. Wei, X., J. M. Decker, H. Liu, Z. Zhang, R. B. Arani, J. M. Kilby, M. S. Saag, X. Wu, G. M. Shaw, and J. C. Kappes. 2002. Emergence of resistant human immunodeficiency virus type 1 in patients receiving fusion inhibitor (T-20) monotherapy. Antimicrob. Agents Chemother. 46:1896–1905.

29. Weiner, M. P., G. L. Costa, W. Schoettlin, J. Cline, E. Mathur, and J. C. Bauer. 1994. Site-directed mutagenesis of double-stranded DNA by the polymerase chain reaction. Gene 151:119–123.

30. Wild, C., T. Oas, C. McDanal, D. Bolognesi, and T. Matthews. 1992. A synthetic peptide inhibitor of human immunodeficiency virus replication: correlation between solution structure and viral inhibition. Proc. Natl. Acad. Sci. USA 89:10537–10541.

ELSEVIER

Studies of non-nucleoside HIV-1 reverse transcriptase inhibitors. Part 2: Synthesis and structure–activity relationships of 2-cyano and 2-hydroxy thiazolidenebenzenesulfonamide derivatives

Naoyuki Masuda,[a,*] Osamu Yamamoto,[a] Masahiro Fujii,[a] Tetsuro Ohgami,[a]
Jiro Fujiyasu,[a] Toru Kontani,[a] Ayako Moritomo,[a] Masaya Orita,[a]
Hiroyuki Kurihara,[a] Hironobu Koga,[a] Shunji Kageyama,[a] Mitsuaki Ohta,[a]
Hiroshi Inoue,[a] Toshifumi Hatta,[a] Masafumi Shintani,[a] Hiroshi Suzuki,[a]
Kenji Sudo,[a] Yasuaki Shimizu,[a] Eiichi Kodama,[b] Masao Matsuoka,[b]
Masatoshi Fujiwara,[c] Tomoyuki Yokota,[c] Shiro Shigeta[d] and Masanori Baba[e]

[a]*Institute for Drug Discovery Research, Yamanouchi Pharmaceutical Co., Ltd, 21 Miyukigaoka, Tsukuba, Ibaraki 305-8585, Japan*
[b]*Laboratory of Virus Immunology, Institute for Virus Research, Kyoto University, 53 Syogoin, Kawaramachi,
Sakyo-ku, Kyoto 606-8507, Japan*
[c]*Rational Drug Design Laboratories, 4-1-1, Misato, Matsukawa-Machi, Fukushima 960-1242, Japan*
[d]*Department of Microbiology, School of Medicine, Fukushima Medical University, 1 Hikarigaoka, Fukushima 960-1295, Japan*
[e]*Division of Antiviral Chemotherapy, Center for Chronic Viral Diseases, Graduate School of Medical and Dental Sciences,
Kagoshima University, 8-35-1 Sakuragaoka, Kagoshima 890-8544, Japan*

Abstract—In a previous study, we described the structure–activity relationships (SARs) for a series of thiazolidenebenzenesulfon-amide derivatives. These compounds were found to be highly potent inhibitors of the wild type (WT) and Y181C mutant reverse transcriptases (RTs) and modest inhibitors of K103N RT. These molecules are thus considered to be a novel class of non-nucleoside HIV-1 RT inhibitors (NNRTIs). In this paper, we have examined the effects of substituents on both the thiazolidene and benzene-sulfonamide moieties. Introduction of a 2-cyanophenyl ring into these moieties significantly enhanced anti-HIV-1 activity, whereas a 2-hydroxyphenyl group endowed potent activity against RTs, including K103N and Y181C mutants. Among the series of molecules examined, 10l and 18b (YM-228855), combinations of 2-cyanophenyl and 4-methyl-5-isopropylthiazole moieties, showed extremely potent anti-HIV-1 activity. The EC_{50} values of 101 and 18b were 0.0017 and 0.0018 μM, respectively. These values were lower than that of efavirenz (3). Compound 11g (YM-215389), a combination of 2-hydroxyphenyl and 4-chloro-5-isopropylthiazole moieties, proved to be the most active against both K103N and Y181C RTs with IC_{50} values of 0.043 and 0.013 μM, respectively.
© 2004 Elsevier Ltd. All rights reserved.

1. Introduction

Reverse transcriptase (RT) is a key enzyme, which plays an essential and multifunctional role in the replication of human immunodeficiency virus type 1 (HIV-1) and thus

considered to be an attractive target for inhibition of HIV-1 replication.[1] Non-nucleoside reverse transcriptase inhibitors (NNRTIs), a group of structurally diverse compounds, have been reported to directly inhibit the enzyme in an allosteric fashion by binding to a pocket near the polymerase active site.[2] To date, many classes of NNRTIs have been identified, and three inhibitors, nevirapine, delavirdine, and efavirenz, have been approved for the treatment of HIV-1 infection. However, NNRTI-containing regimens are compromised by rapid emergence of drug-resistant strains

* Corresponding author. Tel.: +81 298 63 6752; fax: +81 298 52 2971; e-mail: masuda.naoyuki@yamanouchi.co.jp
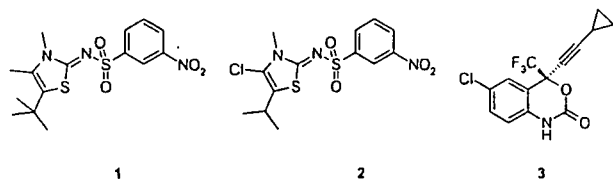
Figure 1. Structures of thiazolidenebenzenesulfonamide derivatives (1, 2) and efavirenz (3).

carrying the amino acid mutations surrounding the NNRTI binding pocket.

The mutation of tyrosine to cysteine at position 181 in HIV-1 RT (Y181C) following treatment with nevirapine or delavirdine has been documented in cell culture experiments.[3] Furthermore, the mutation of lysine to asparagine at position 103 (K103N) is frequently observed in patients who do not respond to the treatment with either NNRTI alone or in combination with other inhibitors.[4] The newest NNRTI, efavirenz (3) has been shown significant clinical efficacy in combination with both protease-containing and protease-sparing regimens.[5] Although the majority of patients receiving efavirenz-containing regimens show a sustained antiviral response, more than 90% of the viruses isolated from the patients whose viral loads have rebounded after an initial drug response have the K103N mutation.[6]

Our previously determined structure–activity relationships (SARs) for a series of thiazolidenebenzenesulfonamide derivatives and docking studies have suggested the importance of a bulky 5-alkyl group on the thiazolidene ring for potent inhibitory activity against Y181C RT.[7] In addition, we found that 3-nitrobenzenesulfonamide derivatives (1, 2) possess potent activity against the wild type (WT) and Y181C RTs, but that their activity against K103N RT was not satisfactory. In this study, we have explored the SARs of substituents in a series of thiazolidenebenzenesulfonamides, in order to identify novel NNRTIs that are capable of inhibiting both K103N and Y181C RT activity and HIV-1 replication (Fig. 1).

2. Chemistry

A series of benzenesulfonamide derivatives (1, 10a–q, 11a–g, 16a, 17a, 18a,b, 19, 20) was synthesized as shown in Schemes 1–4. Cyanobenzenesulfonylchlorides 6n–p were prepared from their corresponding substituted methyl anthranilates (Scheme 1). Sandmeyer reactions of anthranilates 4a–c with ammonia provided saccharins 5a–c.[8] Treatment of saccharins 5a–c with PCl₅ afforded 2-cyanobenzenesulfonylchlorides 6n–p. Compound 4d was converted to the methoxycarbonyl-substituted sulfonylchloride by a one-pot reaction (6q). Condensation of 2-aminothiazoles 8a–c with the substituted sulfonylchlorides 6a–r, followed by selective methylation on the thiazolidene ring of compounds 9a–s, afforded the desired thiazolidenesulfonamide derivatives 1 and 10a–r (Scheme 2).[7] The demethylation of the methoxy deri-
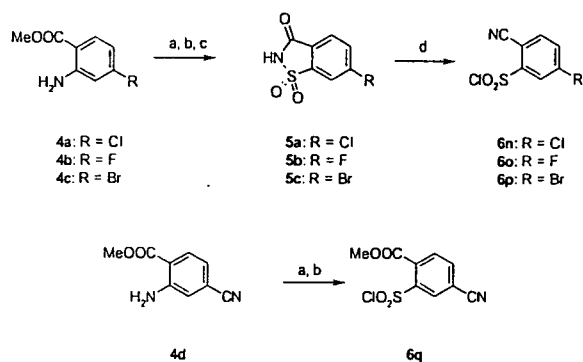
Scheme 1. Reagents and conditions: (a) NaNO₂, HCl/AcOH; (b) SO₂, CuCl, CuCl₂/AcOH–H₂O; (c) NH₃ aq; (d) PCl₅.

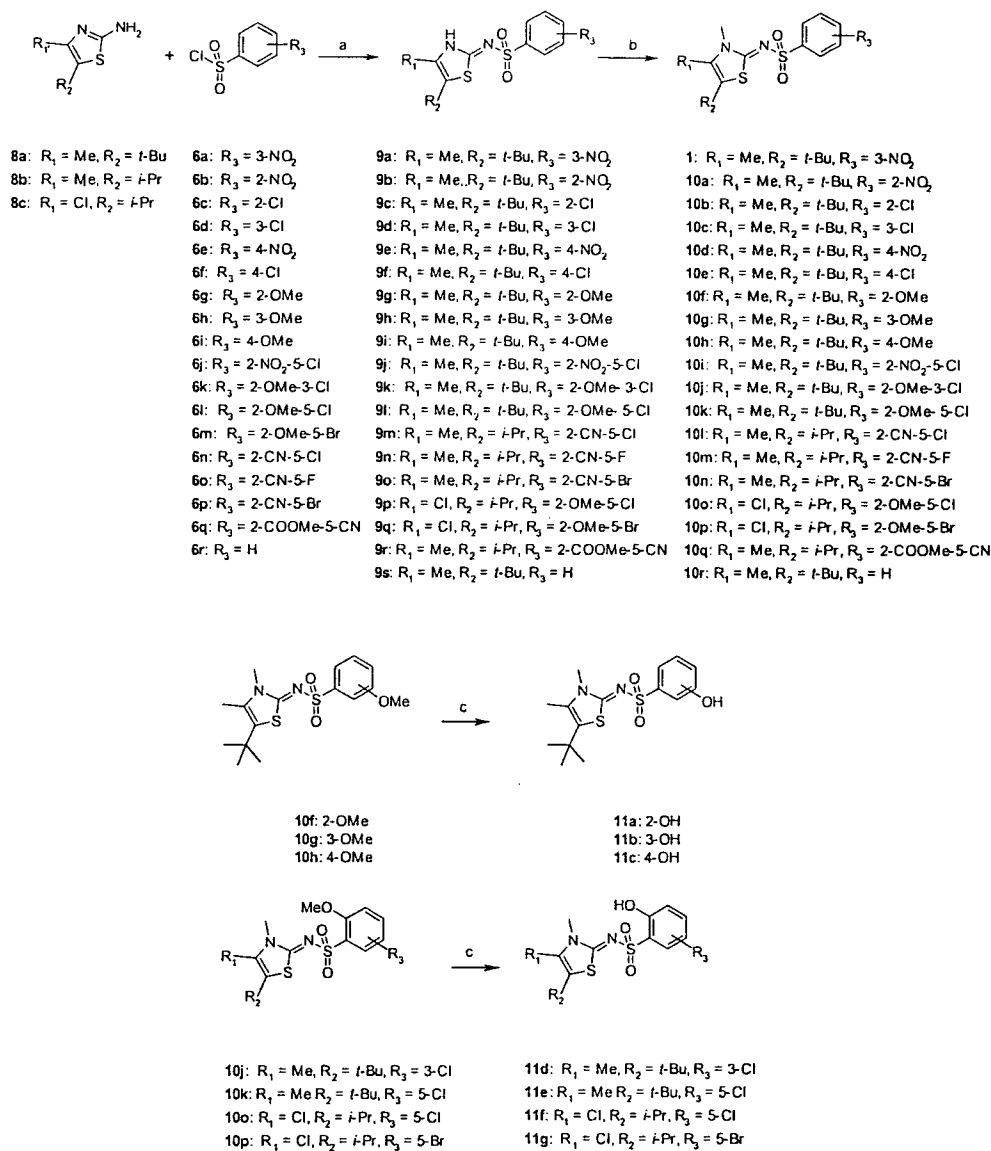vatives (10f–h, j, k, o, p) using BBr₃ provided the corresponding phenol analogues (11a–g).

As shown in Scheme 3, the nitro compound 10i was converted into aniline 12 by catalytic hydrogenation. Aniline 12 was reacted with acetyl chloride or methanesulfonyl chloride to provide acetamide 13 and methanesulfonamide 14, respectively. The triflates 15a and 15b were prepared from the corresponding phenol analogues (11e,f). A palladium-catalyzed carbon monoxide insertion with triflate 15a afforded the methoxycarbonyl derivative 16.[9] Hydrolysis of the ester derivatives (16, 10q) followed by amidation gave the carbamoyl derivatives (17a,b). The cyano derivatives 18a and 18b were obtained by dehydration of compounds 17a and 17b, respectively.

For the synthesis of 2-cyanobenzenesulfonamide derivatives (19, 20), we have efficiently applied palladium-catalyzed cyanation of the aryl triflates with a combination of Pd(dba)₂, dppf, Zn(CN)₂ and Zn powder (Scheme 4).[10] Mono- and di-cyano compounds (19, 20) were obtained by controlling the amount of Zn(CN)₂. Use of 0.6 mol equiv of Zn(CN)₂, which provided 1.2 equiv of cyanide anion, gave the mono-cyano compound 19 through reaction at the triflate group only. With use of 1.6 mol equiv of Zn(CN)₂, the major product was the di-cyano compound 20.

3. Results and discussion

Tables 1–3 summarize the inhibitory activities against the WT, Y181C, and K103N RTs and HIV-1 replication of thiazolidenebenzenesulfonamide derivatives carrying different substituents on the phenyl ring, or at the 4-position on the thiazolidene ring, or both.

We first investigated the effect on the inhibitory activity of substituents on the benzene ring, as shown in Table 1. The RT inhibitory activity of the substituted benzenesulfonamide analogues varied considerably with different substituents. Substituents at the *meta*-position were favorable for the inhibition of RT and HIV-1 replication, and compounds that had a nitro (1) or chloro (10c) group were most potent against all RTs. These

8a: R_1 = Me, R_2 = t-Bu
8b: R_1 = Me, R_2 = i-Pr
8c: R_1 = Cl, R_2 = i-Pr

6a: R_3 = 3-NO$_2$
6b: R_3 = 2-NO$_2$
6c: R_3 = 2-Cl
6d: R_3 = 3-Cl
6e: R_3 = 4-NO$_2$
6f: R_3 = 4-Cl
6g: R_3 = 2-OMe
6h: R_3 = 3-OMe
6i: R_3 = 4-OMe
6j: R_3 = 2-NO$_2$-5-Cl
6k: R_3 = 2-OMe-3-Cl
6l: R_3 = 2-OMe-5-Cl
6m: R_3 = 2-OMe-5-Br
6n: R_3 = 2-CN-5-Cl
6o: R_3 = 2-CN-5-F
6p: R_3 = 2-CN-5-Br
6q: R_3 = 2-COOMe-5-CN
6r: R_3 = H

9a: R_1 = Me, R_2 = t-Bu, R_3 = 3-NO$_2$
9b: R_1 = Me, R_2 = t-Bu, R_3 = 2-NO$_2$
9c: R_1 = Me, R_2 = t-Bu, R_3 = 2-Cl
9d: R_1 = Me, R_2 = t-Bu, R_3 = 3-Cl
9e: R_1 = Me, R_2 = t-Bu, R_3 = 4-NO$_2$
9f: R_1 = Me, R_2 = t-Bu, R_3 = 4-Cl
9g: R_1 = Me, R_2 = t-Bu, R_3 = 2-OMe
9h: R_1 = Me, R_2 = t-Bu, R_3 = 3-OMe
9i: R_1 = Me, R_2 = t-Bu, R_3 = 4-OMe
9j: R_1 = Me, R_2 = t-Bu, R_3 = 2-NO$_2$-5-Cl
9k: R_1 = Me, R_2 = t-Bu, R_3 = 2-OMe-3-Cl
9l: R_1 = Me, R_2 = t-Bu, R_3 = 2-OMe-5-Cl
9m: R_1 = Me, R_2 = i-Pr, R_3 = 2-CN-5-Cl
9n: R_1 = Me, R_2 = i-Pr, R_3 = 2-CN-5-F
9o: R_1 = Me, R_2 = i-Pr, R_3 = 2-CN-5-Br
9p: R_1 = Cl, R_2 = i-Pr, R_3 = 2-OMe-5-Cl
9q: R_1 = Cl, R_2 = i-Pr, R_3 = 2-OMe-5-Br
9r: R_1 = Me, R_2 = i-Pr, R_3 = 2-COOMe-5-CN
9s: R_1 = Me, R_2 = t-Bu, R_3 = H

1: R_1 = Me, R_2 = t-Bu, R_3 = 3-NO$_2$
10a: R_1 = Me, R_2 = t-Bu, R_3 = 2-NO$_2$
10b: R_1 = Me, R_2 = t-Bu, R_3 = 2-Cl
10c: R_1 = Me, R_2 = t-Bu, R_3 = 3-Cl
10d: R_1 = Me, R_2 = t-Bu, R_3 = 4-NO$_2$
10e: R_1 = Me, R_2 = t-Bu, R_3 = 4-Cl
10f: R_1 = Me, R_2 = t-Bu, R_3 = 2-OMe
10g: R_1 = Me, R_2 = t-Bu, R_3 = 3-OMe
10h: R_1 = Me, R_2 = t-Bu, R_3 = 4-OMe
10i: R_1 = Me, R_2 = t-Bu, R_3 = 2-NO$_2$-5-Cl
10j: R_1 = Me, R_2 = t-Bu, R_3 = 2-OMe-3-Cl
10k: R_1 = Me, R_2 = t-Bu, R_3 = 2-OMe-5-Cl
10l: R_1 = Me, R_2 = i-Pr, R_3 = 2-CN-5-Cl
10m: R_1 = Me, R_2 = i-Pr, R_3 = 2-CN-5-F
10n: R_1 = Me, R_2 = i-Pr, R_3 = 2-CN-5-Br
10o: R_1 = Cl, R_2 = i-Pr, R_3 = 2-OMe-5-Cl
10p: R_1 = Cl, R_2 = i-Pr, R_3 = 2-OMe-5-Br
10q: R_1 = Me, R_2 = i-Pr, R_3 = 2-COOMe-5-CN
10r: R_1 = Me, R_2 = t-Bu, R_3 = H

10f: 2-OMe
10g: 3-OMe
10h: 4-OMe

11a: 2-OH
11b: 3-OH
11c: 4-OH

10j: R_1 = Me, R_2 = t-Bu, R_3 = 3-Cl
10k: R_1 = Me R_2 = t-Bu, R_3 = 5-Cl
10o: R_1 = Cl, R_2 = i-Pr, R_3 = 5-Cl
10p: R_1 = Cl, R_2 = i-Pr, R_3 = 5-Br

11d: R_1 = Me, R_2 = t-Bu, R_3 = 3-Cl
11e: R_1 = Me R_2 = t-Bu, R_3 = 5-Cl
11f: R_1 = Cl, R_2 = i-Pr, R_3 = 5-Cl
11g: R_1 = Cl, R_2 = i-Pr, R_3 = 5-Br

Scheme 2. Reagents and conditions: (a) Py; (b) MeI, NaH/THF; (c) BBr$_3$/CH$_2$Cl$_2$.

nitro and chloro substituents also resulted in more potent anti-HIV-1 activity, and compounds **1** and **10c** showed anti-HIV-1 activity with EC$_{50}$ values of 0.085 and 0.20 μM, respectively. In contrast, *ortho-* and *para-* substituted compounds were essentially inactive against the WT RT, with an exception of the *ortho*-hydroxy compound **11a**, which showed a lower IC$_{50}$ value than that of the unsubstituted compound **10r**. Compound **11a** also exhibited moderate anti-HIV-1 activity (EC$_{50}$ = 2.3 μM). Therefore, we concluded that the substitution of a chloro or nitro group at the *meta*-position or a hydroxy group at the *ortho*-position on the benzene ring was favorable for RT inhibition.

We next focused on combinations of an *ortho*-substituent and a *meta*-chloro group, as shown in Table 2. Although the 2-hydroxy-3-chloro derivative (**11d**) was somewhat less active against the WT RT (IC$_{50}$ =

6.3 μM), substitution at the 2-position on a 5-chlorophenyl ring (**11e**, **12**, **18a**), resulted in an enhancement of activity against the RTs. The introduction of an amino group at the 2-position of the phenyl ring (**12**) resulted in a significant improvement of anti-HIV-1 activity but reduced activity against K103N and Y181C RTs, when compared with **10c**. On the other hand, compound **11e** was about 10-fold more potent against the WT and K103N RTs, and 4-fold more potent against Y181C RT, as compared to compound **10c**. The cyano derivative **18a** possessed the most potent antiviral activity (EC$_{50}$ = 0.0083 μM) with a therapeutic index (TI) of >960, but it showed no inhibition of K103N RT. Although the amino and cyano compounds (**12**, **18a**) showed less potent activity against WT RT than the hydroxy compound **11e**, these compounds possessed more potent anti-HIV-1 activity than **11e**. We cannot explain the exact reason for this phenomenon. One possibility,
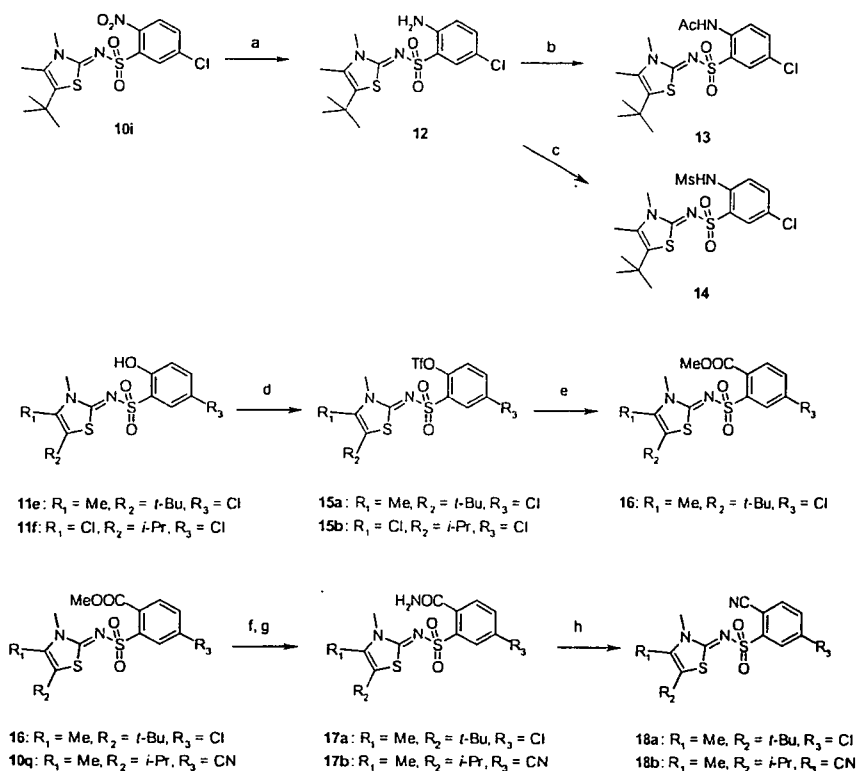
Scheme 3. Reagents and conditions: (a) H₂, Pd–C/EtOH–THF; (b) AcCl, DMAP/Py; (c) MsCl, Et₃N/THF; (d) Tf₂O, 2,6-lutidine/CH₂Cl₂; (e) CO, McOH, Pd(OAc)₂, dppp, Et₃N/DMF; (f) NaOH aq, THF/McOH; (g) NH₄Cl, WSC·HCl, i-Pr₂NEt, HOBt/DMF; (h) POCl₃/DMF.
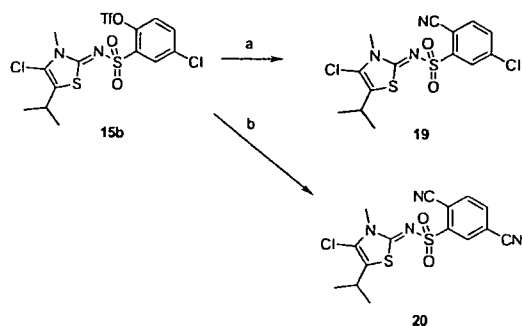
Scheme 4. Reagents and conditions: (a) Zn(CN)₂ (0.6 equiv), Zn, Pd(dba)₂, dppf/DMA; (b) Zn(CN)₂ (1.6 equiv), Zn, Pd(dba)₂, dppf/ DMA.

however, is that the increase in lipophilicity caused by the substitution of the hydroxy group to the amino or cyano group potentiated their cell membrane permeability, which resulted in the increase of anti-HIV-1 activity. We also have to consider other possibilities, such as that the introduction of these groups allow compound stability to be maintained under the assay conditions, or that they acquire the other anti-viral mechanism (inhibition of HIV-protease, integrase, RNaseH, or virus adsorption).

On the other hand, replacement of the cyano group with other electron-withdrawing groups, such as nitro (10i), methoxycarbonyl (16) and carbamoyl (17a), led to loss

of RT inhibition. Substitution of the cyano group with an acetamide or methanesulfonamide group (13, 14), which are known to be bioisosteres of the phenolic hydroxy group, was also detrimental to inhibition with all RTs. Thus, concerning the 5-chlorophenyl derivatives, the introduction of a hydroxy, amino, or cyano group at the 2-position markedly enhanced the inhibition of HIV-1 replication.

We previously reported that compounds with 5-isopropyl-4-methyl- and 4-chloro-5-isopropyl-substituted thiazolidene moieties had increased activity against the WT and Y181C RTs.[7] On the basis of the SARs described in Table 2, we synthesized new compounds with a combination of 2-cyanophenyl or 2-hydroxyphenyl moiety and 5-isopropyl-4-methyl or 4-chloro-5-isopropyl thiazolidene moiety (10l–n, 11f,g, 18b, 19, 20; Table 3). Among these, compound 11f, having both 2-hydroxy-5-chlorophenyl and 4-chlorothiazolidene moieties, was a more potent inhibitor of all the RT enzymes, compared to compound 11e. In addition, compound 11g (YM-215389), which has 5-bromophenyl ring, showed significantly more potent activity against all the RTs, compared to compound 11f. Compound 11g also exhibited strong anti-HIV-1 activity, with an EC₅₀ value of 0.037 μM, and the TI value of 11g exceeded 680. With the exception of compound 10m, the 2-cyanophenyl derivatives (10l, 10n, and 18b), which all have 5-isopropyl-4-methylthiazolidene moieties, exhibited extremely potent anti-HIV-1 activity (EC₅₀ = 0.0017–0.0021 μM), with TIs ranging from 6100 to >15,000. Interestingly,

Table 1. In vitro activities of mono-substituted benzenesulfonamide derivatives
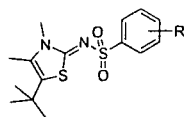
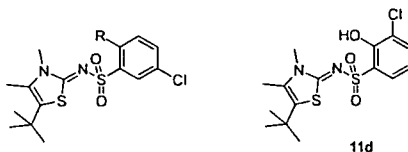| Compounds	R	IC$_{50}$^{a} (μM)			EC$_{50}$^{b} (μM)	CC$_{50}$^{c} (μM)	TI^d
		WT	K103N	Y181C			
1	3-NO$_2$	0.27	13	0.066	0.085	>25	>290
10a	2-NO$_2$	>50	>50	36	>25	>25	—
10b	2-Cl	>10	>10	>10	NT^e	NT^e	
10c	3-Cl	0.30	11	0.044	0.20	>25	>125
10d	4-NO$_2$	>10	>10	>10	NT^e	NT^e	—
10e	4-Cl	>10	>10	>10	NT^e	NT^e	—
10f	2-OMe	50	>50	NT^e	10	>25	>3
10g	3-OMe	8.8	>50	NT^e	11	>25	>2
10h	4-OMe	>10	>10	>10	>25	>25	—
10r	H	4.9	>50	5.1	>25	>25	—
11a	2-OH	1.6	30	0.41	2.3	>25	>11
11b	3-OH	8.8	>50	14	>25	>25	—
11c	4-OH	>10	>10	>10	>25	>25	—

^{a} Compound concentration required to achieve 50% inhibition of recombinant HIV-1 RT activities.
^{b} Compound concentration required to achieve 50% protection of MT-4 cells from HIV-1 induced CPE, as determined by the MTT method.
^{c} Compound concentration required to reduce the viability of mock-infected MT-4 cells, as determined by the MTT method.
^{d} Therapeutic index (CC$_{50}$/EC$_{50}$).
^{e} NT: not tested.

Table 2. In vitro activities of 2-substituted 5-chlorobenzenesulfonamide derivatives

11d

Compounds	R	IC$_{50}$^{a} (μM)			EC$_{50}$^{b} (μM)	CC$_{50}$^{c} (μM)	TI^d
		WT	K103N	Y181C			
10c	H	0.30	11	0.044	0.20	>25	>125
10i	NO$_2$	2.4	>50	NT^e	0.36	22	61
11d		6.3	>50	NT^e	11	>25	>2
11e	OH	0.032	1.1	0.011	0.026	>25	>960
12	NH$_2$	0.19	17	0.11	0.025	>25	>1000
13	NHCOMe	>50	>50	>50	2.7	>25	>9
14	NHSO$_2$Me	>50	>50	>50	>25	>25	··
16	COOMe	>10	>10	10	>25	>25	—
17a	CONH$_2$	>10	>10	>10	NT^e	NT^e	—
18a	CN	0.18	>50	0.069	0.0083	8	>960

^{a} Compound concentration required to achieve 50% inhibition of recombinant HIV-1 RT activities.
^{b} Compound concentration required to achieve 50% protection of MT-4 cells from HIV-1 induced CPE, as determined by the MTT method.
^{c} Compound concentration required to reduce the viability of mock-infected MT-4 cells, as determined by the MTT method.
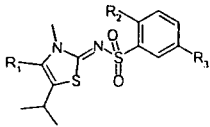^{d} Therapeutic index (CC$_{50}$/EC$_{50}$).
^{e} NT: not tested.

the 2-cyanophenyl and 5-isopropyl-4-methylthiazolid-ene derivatives, 10l and 18b (YM-228855), exhibited strong anti-HIV-1 activity, with EC$_{50}$ values of 0.0017 and 0.0018 μM, respectively, both of which were more potent than that of efavirenz (EC$_{50}$ = 0.0027 μM). The replacement of the 5-chloro or 5-cyano group on the phenyl ring with a 5-bromo group (10n) was tolerable for anti-HIV-1 activity, but this derivative was found to be a modest inhibitor of K103N RT.

We also investigated the substitution of the methyl group at the 4-position of 10l with a chloro group (19, 20), anticipating further increase in RT inhibitory activity and anti-HIV-1 activity. However, this attempt gave slightly less potent compounds than their methyl counterparts. Among the compounds shown in Table 3, compound 11g was the most potent inhibitor against the WT, Y181C, and K103N RTs, with IC$_{50}$ values of 0.0043, 0.043, and 0.013 μM, respectively, and

Table 3. In vitro activities of 5-isopropylthiazolidenesulfonamide derivatives

Compounds	R_1	R_2	R_3	IC_{50}[a] (µM)			EC_{50}[b] (µM)	CC_{50}[c] (µM)	TI[d]
				WT	K103N	Y181C			
10l	Me	CN	Cl	0.011	5.9	0.20	0.0017	>25	>15000
10m	Me	CN	F	0.092	>10	2.1	0.0077	>25	>3200
10n	Me	CN	Br	0.018	3.9	0.26	0.0021	>25	>12,000
11f	Cl	OH	Cl	0.0094	0.17	0.021	0.027	>25	>930
11g (YM-215389)	Cl	OH	Br	0.0043	0.043	0.013	0.037	>25	>680
18b (YM-228855)	Me	CN	CN	0.012	4.1	0.47	0.0018	11	6100
19	Cl	CN	Cl	0.0090	3.7	0.091	0.0047	3.8	810
20	Cl	CN	CN	0.0095	3.0	0.21	0.0036	22	6100
1				0.27	13	0.066	0.085	>25	>290
2				0.077	6.9	0.13	0.048	24	500
Efavirenz (3)				0.0069	0.021	0.0040	0.0027	8.5	3200

[a] Compound concentration required to achieve 50% inhibition of recombinant HIV-1 RT activities.
[b] Compound concentration required to achieve 50% protection of MT-4 cells from HIV-1 induced CPE, as determined by the MTT method.
[c] Compound concentration required to reduce the viability of mock-infected MT-4 cells, as determined by the MTT method.
[d] Therapeutic index (CC_{50}/EC_{50}).

accompanying potent anti-HIV-1 activity (EC_{50}: 0.037 µM). Consequently, the discovery of an effective compound against the WT, K103N, and Y181C mutant RTs as well as HIV-1 replication has been made by the exploration of the optimum combination of substituents on both the thiazole and phenyl rings. This compound is referred to as YM-215389. Further improvement of anti-HIV-1 properties in this series of compounds and their potential use as anti-HIV-1 agents will be reported in due course.

4. Conclusion

In this paper, the synthesis and SARs of thiazolidenebenzenesulfonamide derivatives have been described. An interesting aspect of this study is that both potency and spectrum of thiazolidenebenzenesulfonamides varied, depending on the number and position of the substituents on the phenyl ring. It was found that the combination of a hydroxy or cyano group at the 2-position on the phenyl ring with a 5-isopropylthiazolidene ring improved the inhibitory activities against RT enzymes and HIV-1 replication. The cyano derivatives (10l and 18b) showed extremely potent anti-HIV-1 activity, with EC_{50} values of 0.0017 and 0.0018 µM, respectively. These values were significantly better than that of efavirenz (3). However, the activity of the cyano derivatives against the K103N mutant RT was insufficient. Compound 11g (YM-215389) possessed the most potent activity against the WT, K103N, and Y181C RTs, with IC_{50} values of 0.0043, 0.043, and 0.013 µM, respectively. This compound also strongly inhibited HIV-1 replication in cell cultures (EC_{50} = 0.037 µM). Because of their excellent potency, these thiazolidenebenzenesulfonamide derivatives may have potential and should be further pursued as next-generation NNRTIs.

5. Experimental

5.1. Chemistry

Melting points were determined on a Yanaco micro-melting apparatus or Büchi B-545 melting point apparatus and are uncorrected. Proton magnetic resonance (^{1}H NMR) spectra were obtained in $CDCl_3$ or dimethylsulfoxide-d_6 (DMSO-d_6) using a JEOL JNM-EX90, JNM-EX400, JNM-GX500, or JNM-A500 spectrometer. Chemical shifts were expressed in δ (ppm) values with tetramethylsilane as an internal standard (in NMR description, s: singlet, d: doublet, t: triplet, m: multiplet, br: broad peak). Mass spectra (MS) were recorded on a JEOL JMS-DX300 or a HITACHI M-80 mass spectrometer. Elemental analysis was carried out on Yanaco MT-3 or MT-5 CHN analyzer and a Yokogawa IC7000S Ion Chromatoanalyzer. Chromatographic separations were performed using a silica gel column (Merck Kieselgel 60). Analytical thin-layer chromatography (TLC) was carried out on precoated glass plates (Merck Kieselgel 60F254).

The following known materials were prepared as described in the literature: (6j)[11] or obtained from commercial suppliers (6a–i, 6r). And the preparation of 1, 8a–c, 9a was described in our previous report.[7]

5.1.1. 6-Chloro-1,2-benzisothiazol-3(2H)-one-1,1-dioxide (5a). To solution of 4a (7.42 g, 40 mmol) in acetic acid (45 mL) and concentrated hydrochloric acid (90 mL) was added sodium nitrite (2.90 g, 42 mmol) in water (12 mL) at −5 °C and the solution was stirred at −5 °C for 1 h. To a mixture of copper(II) chloride (5.38 g, 40 mmol) and copper(I) chloride (3.96 g, 40 mmol) in acetic acid (120 mL) and concentrated hydrochloric acid (15 mL), SO_2 gas was bubbled at −5 °C. The suspension of prepared diazonium salt was

added dropwise to the mixture at −10 °C and stirred at room temperature for 3 h. The reaction mixture was poured into water and 28% aqueous ammonia solution (500 mL) was added under ice-bath cooling. The resulting mixture was extracted with chloroform and washed with saturated aqueous sodium hydrogen carbonate solution. The organic layer was dried over anhydrous sodium sulfate and solvent was removed under reduced pressure to give 5a (3.90 g, 45%) as a colorless powder. ¹H NMR (DMSO-d_6) δ: 7.97 (3H, m, benzene), 8.43 (1H, br s, NH); FAB-MS *m/z*: 218 (M⁺+1).

The following compounds were obtained in the same manner.

5.1.2. 6-Fluoro-1,2-benzisothiazol-3(2*H*)-one-1,1-dioxide (5b). 31% yield; ¹H NMR (DMSO-d_6) δ: 7.57 (1H, m, benzene), 7.82 (2H, m, benzene), 7.90 (1H, m, NH); FAB-MS *m/z*: 200 (M⁻−1).

5.1.3. 6-Bromo-1,2-benzisothiazol-3(2*H*)-one-1,1-dioxide (5c). 56% yield; ¹H NMR (DMSO-d_6) δ: 7.80 (1H, br s, NH), 7.87 (1H, d, *J* = 8.3 Hz, benzene), 8.09 (1H, dd, *J* = 1.5, 8.3 Hz, benzene), 8.51 (1H, d, *J* = 1.5 Hz, benzene); FAB-MS *m/z*: 263 (M⁺+1).

5.1.4. 5-Chloro-2-cyanobenzenesulfonyl chloride (6n). A mixture of 5a (3.90 g, 18.0 mmol) and phosphorus pentachloride (22.4 g, 90.0 mmol) was heated to 120 °C and stirred for 7 h. The reaction mixture was poured into ice-water. The resulting mixture was extracted with ethyl acetate and washed with saturated aqueous sodium hydrogen carbonate solution. The organic layer was dried over anhydrous sodium sulfate and solvent was removed under reduced pressure to give 6n (2.89 g, 68%) as a pale yellow powder. This crude product was used for next step without further purification.

The following compounds were obtained in the same manner.

5.1.5. 5-Fluoro-2-cyanobenzenesulfonyl chloride (6o). 54% yield; ¹H NMR (DMSO-d_6) δ: 7.40 (1H, dt, *J* = 3.6, 11.2 Hz, benzene), 7.59 (1H, dd, *J* = 3.6, 12.0 Hz, benzene), 7.92 (1H, dd, *J* = 6.8, 11.2 Hz, benzene); EI-MS *m/z*: 219 (M⁺).

5.1.6. 5-Bromo-2-cyanobenzenesulfonyl chloride (6p). Without isolation.

5.1.7. Methyl 2-chlorosulfonyl-4-cyanobenzoate (6q). Sodium nitrite (5.10 g, 73.5 mmol) in water (25 mL) was added to solution of 4d (12.3 g, 70 mmol) in concentrated hydrochloric acid (120 mL) at −5 °C and the solution was stirred at −5 °C for 1.5 h. To a mixture of copper(II) chloride dihydrate (2.60 g, 15.0 mmol) in acetic acid (200 mL), SO₂ gas was bubbled at −5 °C. The suspension of prepared diazonium salt was added dropwise to the mixture at −10 °C and stirred at room temperature for 3 h. The reaction mixture was poured into water. The resulting precipitate was collected by filtration and washed with water. The precipitate was

dried under reduced pressure to give 6q (19.0 g, quantitative) as a colorless powder. ¹H NMR (DMSO-d_6) δ: 3.75 (3H, s, CH₃ of COOMe), 7.52 (1H, d, *J* = 8.1 Hz, benzene), 7.87 (1H, dd, *J* = 1.5, 8.1 Hz, benzene), 8.03 (1H, d, *J* = 1.5 Hz, benzene); EI-MS *m/z*: 259 (M⁺).

5.1.8. *N*-(5-*tert*-Butyl-4-methyl-1,3-thiazol-2-yl)-2-nitrobenzenesulfonamide (9b). A solution of 8a. hydrochloride (8.00 g, 38.7 mmol) in pyridine (100 mL) was added 6b (10.3 g, 46.4 mmol) and the solution was stirred at room temperature for 12 h. The reaction mixture was poured into water. The resulting mixture was extracted with ethyl acetate and washed with saturated aqueous sodium hydrogen carbonate solution, 1 M hydrochloric acid and brine. The organic layer was dried over anhydrous sodium sulfate and solvent was removed under reduced pressure. The residue was purified by silica gel column chromatography (ethyl acetate–hexane) to give 9b (10.89 g, 79%) as an orange solid. ¹H NMR (DMSO-d_6) δ: 1.30 (9H, s, *t*-Bu), 2.18 (3H, s, 4-Me), 7.80 (2H, m, benzene), 7.87 (1H, m, benzene), 8.03 (1H, m, benzene), 12.65 (1H, br s, NH); FAB-MS *m/z*: 356 (M⁺+1).

The following compounds were obtained in the same manner.

5.1.9. *N*-(5-*tert*-Butyl-4-methyl-1,3-thiazol-2-yl)-2-chlorobenzenesulfonamide (9c). 34% yield; ¹H NMR (DMSO-d_6) δ: 1.30 (9H, s, CH₃ of *t*-Bu), 2.16 (3H, s, 4-Me), 8.03 (2H, d, *J* = 8.8 Hz, benzene), 8.36 (2H, d, *J* = 8.8 Hz, benzene), 12.58 (1H, br s, NH); FAB-MS *m/z*: 345 (M⁺+1).

5.1.10. *N*-(5-*tert*-Butyl-4-methyl-1,3-thiazol-2-yl)-3-chlorobenzenesulfonamide (9d). 99% yield; ¹H NMR (DMSO-d_6) δ: 1.29 (9H, s, CH₃ of *t*-Bu), 2.16 (3H, s, 4-Me), 7.58 (1H, t, *J* = 7.8 Hz, benzene), 7.67 (1H, br d, *J* = 7.8 Hz, benzene), 7.74 (1H, br s, benzene), 7.75 (1H, br d, *J* = 7.8 Hz, benzene), 12.46 (1H, br s, NH); FAB-MS *m/z*: 345 (M⁺+1).

5.1.11. *N*-(5-*tert*-Butyl-4-methyl-1,3-thiazol-2-yl)-4-nitrobenzenesulfonamide (9e). 85% yield; ¹H NMR (DMSO-d_6) δ: 1.30 (9H, s, CH₃ of *t*-Bu), 2.16 (3H, s, 4-Me), 8.03 (2H, d, *J* = 8.8 Hz, benzene), 8.36 (2H, d, *J* = 8.8 Hz, benzene), 12.58 (1H, br s, NH); FAB-MS *m/z*: 356 (M⁺+1).

5.1.12. *N*-(5-*tert*-Butyl-4-methyl-1,3-thiazol-2-yl)-4-chlorobenzenesulfonamide (9f). 78% yield; ¹H NMR (DMSO-d_6) δ: 1.29 (9H, s, CH₃ of *t*-Bu), 2.15 (3H, s, 4-Me), 7.60 (2H, d, *J* = 7.5 Hz, benzene), 7.78 (2H, d, *J* = 7.5 Hz, benzene), 12.42 (1H, br s, NH); FAB-MS *m/z*: 345 (M⁺+1).

5.1.13. *N*-(5-*tert*-Butyl-4-methyl-1,3-thiazol-2-yl)-2-methoxybenzenesulfonamide (9g). 50% yield; ¹H NMR (DMSO-d_6) δ: 1.31 (9H, s, CH₃ of *t*-Bu), 2.15 (3H, s, 4-Me), 3.73 (3H, s, MeO), 7.03 (1H, t, *J* = 7.5 Hz, benzene), 7.13 (1H, d, *J* = 7.5 Hz, benzene), 7.50 (2H, m, benzene), 12.14 (1H, br s, NH); FAB-MS *m/z*: 341 (M⁺+1).

5.1.14. N-(5-tert-Butyl-4-methyl-1,3-thiazol-2-yl)-3-methoxybenzenesulfonamide (9h). 61% yield; ^{1}H NMR (DMSO-d_6) δ: 1.29 (9H, s, CH$_3$ of t-Bu), 1.98 (3H, s, 4-Me), 3.80 (3H, s, MeO), 7.14 (1H, dd, J = 2.5, 8.3 Hz, benzene), 7.26 (1H, t, J = 2.5 Hz, benzene), 7.36 (1H, br d, J = 7.8 Hz, benzene), 7.45 (1H, t, J = 7.8 Hz, benzene), 12.34 (1H, br s, benzene); FAB-MS m/z: 341 (M$^+$+1).

5.1.15. N-(5-tert-Butyl-4-methyl-1,3-thiazol-2-yl)-4-methoxybenzenesulfonamide (9i). Without isolation.

5.1.16.　　　N-(5-tert-Butyl-4-methyl-1,3-thiazol-2-yl)-5-chloro-2-nitrobenzenesulfonamide (9j). 41% yield; ^{1}H NMR (DMSO-d_6) δ: 1.30 (9H, s, CH$_3$ of t-Bu), 2.20 (3H, s, 4-Me), 7.91 (1H, dd, J = 2.0, 8.3 Hz, benzene), 7.98 (1H, d, J = 2.0 Hz, benzene), 7.99 (1H, d, J = 8.8 Hz, benzene), 12.76 (1H, br s, NH); FAB-MS m/z: 390 (M$^+$+1).

5.1.17.　　　N-(5-tert-Butyl-4-methyl-1,3-thiazol-2-yl)-3-chloro-2-methoxybenzenesulfonamide　　(9k). Without isolation.

5.1.18.　　　N-(5-tert-Butyl-4-methyl-1,3-thiazol-2-yl)-5-chloro-2-methoxybenzenesulfonamide (9l). 94% yield; ^{1}H NMR (DMSO-d_6) δ: 1.32 (9H, s, CH$_3$ of t-Bu), 2.17 (3H, s, 4-Me), 3.74 (3H, s, MeO), 7.18 (1H, d, J = 8.8 Hz, benzene), 7.59 (1H, dd, J = 2.9, 8.8 Hz, benzene), 7.73 (1H, d, J = 2.9 Hz, benzene), 12.30 (1H, br s, NH); FAB-MS m/z: 375 (M$^+$+1).

5.1.19.　5-Chloro-2-cyano-N-(5-isopropyl-4-methyl-1,3-thiazol-2-yl)benzenesulfonamide (9m). 13% yield. ^{1}H NMR (DMSO-d_6) δ: 1.14 (6H, d, J = 6.8 Hz, CH$_3$ of i-Pr), 2.06 (3H, s, 4-Me), 3.11 (1H, heptet, J = 6.8 Hz, CH of i-Pr), 7.88 (1H, dd, J = 2.5, 8.3 Hz, benzene), 8.00 (1H, d, J = 2.5 Hz, benzene), 8.09 (1H, d, J = 8.3 Hz, benzene), 12.83 (1H, br s, NH); FAB-MS m/z: 356 (M$^+$+1).

5.1.20.　　5-Fluoro-2-cyano-N-(5-isopropyl-4-methyl-1,3-thiazol-2-yl)benzenesulfonamide (9n). 20% yield; ^{1}H NMR (DMSO-d_6) δ: 1.14 (6H, d, J = 6.9 Hz, CH$_3$ of i-Pr), 2.06 (3H, s, 4-Me), 3.11 (1H, heptet, J = 6.9 Hz, CH of i-Pr), 7.67 (1H, dt, J = 1.9, 8.8 Hz, benzene), 7.82 (1H, dd, J = 1.9, 8.8 Hz, benzene), 8.16 (1H, dd, J = 5.4, 8.8 Hz, benzene), 12.82 (1H, br s, NH); FAB-MS m/z: 340 (M$^+$+1).

5.1.21.　　5-Bromo-2-cyano-N-(5-isopropyl-4-methyl-1,3-thiazol-2-yl)benzenesulfonamide (9o). 27% yield from 8b; ^{1}H NMR (DMSO-d_6) δ: 1.14 (6H, d, J = 6.8 Hz, CH$_3$ of i-Pr), 2.06 (3H, s, 4-Me), 3.11 (1H, heptet, J = 6.8 Hz, CH of i-Pr), 8.01 (2H, m, benzene), 8.13 (1H, d, J = 1.4 Hz, benzene), 12.84 (1H, br s, NH).; FAB-MS m/z: 400 (M$^+$+1).

5.1.22.　　　N-(4-Chloro-5-isopropyl-1,3-thiazol-2-yl)-5-chloro-2-methoxybenzenesulfonamide (9p). 22% yield; ^{1}H NMR (CDCl$_3$) δ: 1.25 (6H, d, J = 7.0 Hz, CH$_3$ of i-Pr), 2.67 (1H, br s, NH), 3.16 (1H, heptet, J = 7.0 Hz, CH of i-Pr), 3.87 (3H, s, MeO), 6.94 (1H,

d, J = 8.8 Hz, benzene), 7.46 (1H, dd, J = 2.4, 8.8 Hz, benzene), 7.94 (1H, d, J = 2.4 Hz, benzene); FAB-MS m/z: 381 (M$^+$+1).

5.1.23.　　　N-(4-Chloro-5-isopropyl-1,3-thiazol-2-yl)-5-bromo-2-methoxybenzenesulfonamide (9q). 59% yield;. ^{1}H NMR (DMSO-d_6) δ: 1.20 (6H, d, J = 6.8 Hz, CH$_3$ of i-Pr), 3.12 (1H, heptet, J = 6.8 Hz, CH of i-Pr), 3.76 (3H, s, MeO), 7.14 (1H, d, J = 9.0 Hz, benzene), 7.79 (1H, dd, J = 2.6, 9.0 Hz, benzene), 7.87 (1H, d, J = 2.6 Hz, benzene); FAB-MS m/z: 427 (M$^+$+1).

5.1.24. Methyl 4-cyano-2-{[(5-isopropyl-4-methyl-1,3-thiazol-2-yl)amino]sulfonyl}benzoate (9r). 68% yield; ^{1}H NMR (DMSO-d_6) δ: 1.15 (6H, d, J = 6.9 Hz, CH$_3$ of i-Pr), 2.07 (3H, s, 4-Me), 3.11 (1H, heptet, J = 6.9 Hz, CH of i-Pr), 3.80 (3H, s, CH$_3$ of COOMe), 7.78 (1H, d, J = 7.8 Hz, benzene), 8.14 (1H, dd, J = 1.4, 7.8 Hz, benzene), 8.28 (1H, d, J = 1.4 Hz, benzene), 12.59 (1H, br s, NH); FAB-MS m/z: 380 (M$^+$+1).

5.1.25.　　N-(5-tert-Butyl-4-methyl-1,3-thiazol-2-yl)benzenesulfonamide (9s). 61% yield; ^{1}H NMR (DMSO-d_6) δ: 1.28 (9H, s, CH$_3$ of t-Bu), 2.14 (3H, s, 4-Me), 7.54 (3H, m, benzene), 7.78 (2H, m, benzene), 12.32 (1H, br s, NH); FAB-MS m/z: 311 (M$^+$+1).

5.1.26.　　N-(5-tert-Butyl-3,4-dimethyl-1,3-thiazol-2(3H)-ylidene)-2-nitrobenzenesulfonamide (10a). To a solution of 9b (10.89 g, 30.6 mmol) in tetrahydrofuran (100 mL) was added sodium hydride (60% dispersion in mineral oil: 1.47 g, 36.8 mmol) and iodomethane (5.7 mL, 91.8 mmol) under ice-bath cooling. The solution was warmed to room temperature and stirred for 12 h. The reaction mixture was poured into ice-water and extracted with ethyl acetate. The organic layer was washed with brine, and then dried over anhydrous sodium sulfate. The solvent was removed under reduced pressure and the residue was purified by silica gel column chromatography (chloroform) and recrystalized from methanol to give 10a (7.01 g, 62%) as a yellow powder. Mp 138–139 °C. ^{1}H NMR (CDCl$_3$) δ: 1.36 (9H, s, CH$_3$ of t-Bu), 2.28 (3H, s, 4-Me), 3.45 (3H, s, 3-Me), 7.61 (3H, m, benzene), 8.25 (1H, m, benzene); FAB-MS m/z: 370 (M$^+$+1). Anal. Calcd for C$_{15}$H$_{19}$N$_3$O$_4$S$_2$: C, 48.76; H, 5.18; N, 11.37; S, 17.36. Found: C, 48.76; H, 4.99; N, 11.38; S, 17.69.

The following compounds were obtained in the same manner.

5.1.27.　　N-(5-tert-Butyl-3,4-dimethyl-1,3-thiazol-2(3H)-ylidene)-2-chlorobenzenesulfonamide (10b). 86% yield; mp 153–155 °C (ethyl acetate–benzene).^{1}H NMR (CDCl$_3$) δ: 1.33 (9H, s, CH$_3$ of t-Bu), 2.27 (3H, s, 4-Me), 3.47 (3H, s, 3-Me), 7.46 (3H, m, benzene), 8.23 (1H, m, benzene); FAB-MS m/z: 359 (M$^+$+1). Anal. Calcd for C$_{15}$H$_{19}$ClN$_2$O$_2$S$_2$: C, 50.20; H, 5.34; N, 7.81; S, 17.87; Cl, 9.88. Found: C, 50.15; H, 5.17; N, 7.82; S, 17.80; Cl, 9.75.

5.1.28.　　N-(5-tert-Butyl-3,4-dimethyl-1,3-thiazol-2(3H)-ylidene)-3-chlorobenzenesulfonamide (10c). 90% yield;

mp 138–139 °C (chloroform). ^{1}H NMR (DMSO-d_6) δ: 1.31 (9H, s, CH$_3$ of t-Bu), 2.28 (3H, s, 4-Me), 3.42 (3H, s, 3-Me), 7.57 (1H, dd, J = 7.8, 8.3 Hz, benzene), 7.66 (1H, ddd, J = 1.0, 2.0, 8.3 Hz, benzene), 7.79 (1H, br s, benzene), 7.80 (1H, br d, J = 7.8 Hz, benzene); FAB-MS m/z: 359 (M$^+$+1). Anal. Calcd for C$_{15}$H$_{19}$ClN$_2$O$_2$S$_2$Cl: C, 50.20; H, 5.34; N, 7.81; S, 17.87; Cl, 9.88. Found: C, 50.01; H, 5.26; N, 7.76; S, 18.00; Cl, 10.04.

5.1.29. **N-(5-$tert$-Butyl-3,4-dimethyl-1,3-thiazol-2(3H)-ylidene)-4-nitrobenzenesulfonamide (10d).** 50% yield; mp 184–185 °C (ethyl acetate–hexane). ^{1}H NMR (CDCl$_3$) δ: 1.37 (9H, s, CH$_3$ of t-Bu), 2.27 (3H, s, 4-Me), 3.46 (3H, s, 3-Me), 8.15 (2H, dt, J = 2.4, 8.8 Hz, benzene), 8.29 (2H, dt, J = 2.4, 8.8 Hz, benzene); FAB-MS m/z: 370 (M$^+$+1). Anal. Calcd for C$_{15}$H$_{19}$N$_3$O$_4$S$_2$: C, 48.76; H, 5.18; N, 11.37; S, 17.36. Found: C, 48.70; H, 4.98; N, 11.51; S, 17.43.

5.1.30. **N-(5-$tert$-Butyl-3,4-dimethyl-1,3-thiazol-2(3H)-ylidene)-4-chlorobenzenesulfonamide (10e).** 50% yield; mp 157–158 °C (ethyl acetate–hexane). ^{1}H NMR (CDCl$_3$) δ: 1.36 (9H, s, CH$_3$ of t-Bu), 2.26 (3H, s, 4-Me), 3.43 (3H, s, 3-Me), 7.41 (2H, dt, J = 2.4, 8.8 Hz, benzene), 7.91 (2H, dt, J = 2.4, 8.8 Hz, benzene); FAB-MS m/z: 359 (M$^+$+1). Anal. Calcd for C$_{15}$H$_{19}$ClN$_2$O$_2$S$_2$: C, 50.20; H, 5.34; N, 7.81; S, 17.87; Cl, 9.88. Found: C, 50.01; H, 5.10; N, 7.87; S, 17.86; Cl, 9.89.

5.1.31. **N-(5-$tert$-Butyl-3,4-dimethyl-1,3-thiazol-2(3H)-ylidene)-2-methoxybenzenesulfonamide (10f).** 20% yield; mp 197–198 °C (diethyl ether–hexane). ^{1}H NMR (DMSO-d_6) δ: 1.33 (9H, s, CH$_3$ of t-Bu), 2.28 (3H, s, 4-Me), 3.37 (3H, s, 3-Me), 3.73 (3H, s, MeO), 7.03 (1H, t, J = 7.9 Hz, benzene), 7.14 (1H, d, J = 8.3 Hz, benzene), 7.52 (1H, dt, J = 1.5, 7.9 Hz, benzene), 7.79 (1H, dd, J = 1.5 Hz, benzene); FAB-MS m/z: 355 (M$^+$+1). Anal. Calcd for C$_{16}$H$_{22}$N$_2$O$_3$S$_2$·0.1CHCl$_3$: C, 52.77; H, 6.08; N, 7.65; S, 17.50; Cl, 2.90. Found: C, 52.84; H, 5.98; N, 7.59; S, 17.56; Cl, 2.50.

5.1.32. **N-(5-$tert$-Butyl-3,4-dimethyl-1,3-thiazol-2(3H)-ylidene)-3-methoxybenzenesulfonamide (10g).** 76% yield; mp 192–193 °C (diethyl ether). ^{1}H NMR (DMSO-d_6) δ 1.31 (9H, s, CH$_3$ of t-Bu), 2.27 (3H, s, 4-Me), 3.40 (3H, s, 3-Me), 3.81 (3H, s, MeO), 7.14 (1H, ddd, J = 1.0, 2.5, 7.8 Hz, benzene), 7.29 (1H, t, J = 2.5 Hz, benzene), 7.39 (1H, br d, J = 7.8 Hz, benzene), 7.44 (1H, t, J = 7.8 Hz, benzene); FAB-MS m/z: 355 (M$^+$+1). Anal. Calcd for C$_{16}$H$_{22}$N$_2$O$_3$S$_2$: C, 54.21; H, 6.26; N, 7.90; S, 18.09. Found: C, 54.31; H, 6.25; N, 7.86; S, 18.17.

5.1.33. **N-(5-$tert$-Butyl-3,4-dimethyl-1,3-thiazol-2(3H)-ylidene)-4-methoxybenzenesulfonamide (10h).** 81% yield from 8a; mp 181–183 °C (ethyl acetate–hexane). ^{1}H NMR (CDCl$_3$) δ: 1.34 (9H, s, CH$_3$ of t-Bu), 2.24 (3H, s, 4-Me), 3.42 (3H, s, 3-Me), 3.87 (3H, s, MeO), 6.92 (2H, d, J = 8.6 Hz, benzene), 7.91 (2H, d, J = 8.6 Hz, benzene); FAB-MS m/z: 355 (M$^+$+1). Anal. Calcd for C$_{16}$H$_{22}$N$_2$O$_3$S$_2$: C, 54.21; H, 6.26; N, 7.90; S, 18.09. Found: C, 54.23; H, 6.18; N, 7.89; S, 17.98.

5.1.34. **N-(5-$tert$-Butyl-3,4-dimethyl-1,3-thiazol-2(3H)-ylidene)-5-chloro-2-nitrobenzenesulfonamide (10i).** 49% yield; mp 204–205 °C (acetonitrile). ^{1}H NMR (DMSO-d_6) δ: 1.33 (9H, s, CH$_3$ of t-Bu), 2.31 (3H, s, 4-Me), 3.45 (3H, s, 3-Me), 7.91 (1H, dd, J = 1.9, 8.3 Hz, benzene), 7.98 (1H, d, J = 8.3 Hz, benzene), 8.01 (1H, d, J = 1.9 Hz, benzene); FAB-MS m/z: 404 (M$^+$+1). Anal. Calcd for C$_{15}$H$_{18}$ClN$_3$O$_4$S$_2$: C, 44.60; H, 4.49; N, 10.40; S, 15.88; Cl, 8.78. Found: C, 44.44; H, 4.41; N, 10.34; S, 16.03; Cl, 8.82.

5.1.35. **N-(5-$tert$-Butyl-3,4-dimethyl-1,3-thiazol-2(3H)-ylidene)-3-chloro-2-methoxybenzenesulfonamide (10j).** 60% yield from 8a; ^{1}H NMR (DMSO-d_6) δ: 1.22 (9H, s, CH$_3$ of t-Bu), 2.22 (3H, s, 4-Me), 3.35 (3H, s, 3-Me), 3.73 (3H, s, MeO), 7.38 (1H, dd, J = 7.8, 8.3 Hz, benzene), 7.77 (1H, dd, J = 1.5, 8.3 Hz, benzene), 7.88 (1H, dd, J = 1.5, 7.8 Hz, benzene); FAB-MS m/z: 388 (M$^+$+1).

5.1.36. **N-(5-$tert$-Butyl-3,4-dimethyl-1,3-thiazol-2(3H)-ylidene)-5-chloro-2-methoxybenzenesulfonamide (10k).** 81% yield; ^{1}H NMR (DMSO-d_6) δ: 1.34 (9H, s, CH$_3$ of t-Bu), 2.29 (3H, s, 4-Me), 3.38 (3H, s, 3-Me), 3.73 (3H, s, MeO), 7.19 (1H, d, J = 8.8 Hz, benzene), 7.59 (1H, dd, J = 2.5, 8.8 Hz, benzene), 7.73 (1H, d, J = 2.5 Hz, benzene); FAB-MS m/z: 388 (M$^+$+1).

5.1.37. **5-Chloro-2-cyano-N-(5-isopropyl-3,4-dimethyl-1,3-thiazol-2(3H)-ylidene)benzenesulfonamide (10l).** 63% yield; mp 180–182 °C. ^{1}H NMR (DMSO-d_6) δ: 1.15 (6H, d, J = 6.9 Hz, CH$_3$ of i-Pr), 2.19 (3H, s, 4-Me), 3.22 (1H, heptet, J = 6.9 Hz, CH of i-Pr), 3.48 (3H, s, 3-Me), 7.88 (1H, dd, J = 1.9, 8.3 Hz, benzene), 8.02 (1H, d, J = 1.9 Hz, benzene), 8.10 (1H, d, J = 8.3 Hz, benzene); FAB-MS m/z: 370 (M$^+$+1). Anal. Calcd for C$_{15}$H$_{16}$ClN$_3$O$_2$S$_2$: C, 48.71; H, 4.36; N, 11.36; S, 17.34; Cl, 9.58. Found: C, 48.43; H, 4.24; N, 11.33; S, 17.45; Cl, 9.38.

5.1.38. **5-Fluoro-2-cyano-N-(5-isopropyl-3,4-dimethyl-1,3-thiazol-2(3H)-ylidene)benzenesulfonamide (10m).** 81% yield; mp 184–186 °C (methanol–chloroform). ^{1}H NMR (DMSO-d_6) δ: 1.14 (6H, d, J = 6.8 Hz, CH$_3$ of i-Pr), 2.19 (3H, s, 4-Me), 3.20 (1H, heptet, J = 6.8 Hz, CH of i-Pr), 3.49 (3H, s, 3-Me), 7.66 (1H, dt, J = 2.9, 8.3 Hz, benzene), 7.85 (1H, dd, J = 2.5, 8.3 Hz, benzene), 8.16 (1H, dd, J = 5.3, 8.8 Hz, benzene); FAB-MS m/z: 354 (M$^+$+1). Anal. Calcd for C$_{15}$H$_{16}$FN$_3$O$_2$S$_2$: C, 50.97; H, 4.56; N, 11.89; S, 18.15; F, 5.38. Found: C, 51.05; H, 4.60; N, 11.76; S, 18.09; F, 5.63.

5.1.39. **5-Bromo-2-cyano-N-(5-isopropyl-3,4-dimethyl-1,3-thiazol-2(3H)-ylidene)benzenesulfonamide (10n).** 56% yield; mp 179–181 °C (isopropanol). ^{1}H NMR (DMSO-d_6) δ: 1.15 (6H, d, J = 6.9 Hz, CH$_3$ of i-Pr), 2.18 (3H, s, 4-Me), 3.22 (1H, heptet, J = 6.9 Hz, CH of i-Pr), 3.48 (3H, s, 3-Me), 8.01 (2H, m, benzene), 8.14 (1H, d, J = 1.0 Hz, benzene); FAB-MS m/z: 414 (M$^+$+1). Anal. Calcd for C$_{15}$H$_{16}$BrN$_3$O$_2$S$_2$: C, 43.48; H, 3.89; N, 10.14; S, 15.48; Br, 19.28. Found: C, 43.50; H, 3.70; N, 10.07; S, 15.51; Br, 18.91.

5.1.40. **5-Chloro-*N*-(4-chloro-5-isopropyl-3-methyl-1,3-thiazol-2(3*H*)-ylidene)-2-methoxybenzenesulfonamide (10o).** 60% yield; ¹H NMR (DMSO-*d₆*) *δ*: 1.23 (6H, d, *J* = 6.8 Hz, CH₃ of *i*-Pr), 3.20 (1H, heptet, *J* = 6.8 Hz, CH of *i*-Pr), 3.43 (3H, s, 3-Me), 3.74 (3H, s, MeO), 7.22 (1H, d, *J* = 8.8 Hz, benzene), 7.63 (1H, dd, *J* = 2.5, 8.8 Hz, benzene), 7.76 (1H, d, *J* = 2.4 Hz, benzene); FAB-MS *m/z*: 395 (M⁺+1).

5.1.41. **5-Bromo-*N*-(4-chloro-5-isopropyl-3-methyl-1,3-thiazol-2(3*H*)-ylidene)-2-methoxybenzenesulfonamide (10p).** 73% yield; ¹H NMR (CDCl₃) *δ*: 1.26 (6H, d, *J* = 6.8 Hz, CH₃ of *i*-Pr), 3.22 (1H, heptet, *J* = 6.8 Hz, CH of *i*-Pr), 3.51 (3H, s, 3-Me), 3.82 (3H, s, MeO), 6.85 (1H, d, *J* = 8.8 Hz, benzene), 7.55 (1H, dd, *J* = 2.4, 8.8 Hz, benzene), 8.16 (1H, d, *J* = 2.4 Hz, benzene); FAB-MS *m/z*: 439 (M⁺+1).

5.1.42. Methyl 4-cyano-2-{[(5-isopropyl-3,4-dimethyl-1,3-thiazol-2(3*H*)-ylidene)amino]sulfonyl}benzoate (10q). 37% yield; mp 224–226 °C (isopropanol–diethyl ether). ¹H NMR (DMSO-*d₆*) *δ*: 1.15 (6H, d, *J* = 6.9 Hz, CH₃ of *i*-Pr), 3.22 (1H, heptet, *J* = 6.9 Hz, CH of *i*-Pr), 2.19 (3H, s, 4-Me), 3.44 (3H, s, 3-Me), 3.81 (3H, s, MeO), 7.78 (1H, d, *J* = 7.8 Hz, benzene), 8.14 (1H, dd, *J* = 1.5, 7.8 Hz, benzene), 8.33 (1H, d, *J* = 1.5 Hz, benzene); FAB-MS *m/z*: 394 (M⁺+1). Anal. Calcd for C₁₇H₁₉N₃O₄S₂: C, 51.89; H, 4.87; N, 10.68; S, 16.30. Found: C, 51.65; H, 4.79; N, 10.72; S, 16.03.

5.1.43. ***N*-(5-*tert*-Butyl-3,4-dimethyl-1,3-thiazol-2(3*H*)-ylidene)benzenesulfonamide (10r).** 95% yield; mp 188–189 °C (ethyl acetate–hexane). ¹H NMR (DMSO-*d₆*) *δ*: 1.31 (9H, s, CH₃ of *t*-Bu), 2.26 (3H, s, 4-Me), 3.40 (3H, s, 3-Me), 7.54 (3H, m, benzene), 7.82 (2H, m, benzene); FAB-MS *m/z*: 325 (M⁺+1). Anal. Calcd for C₁₅H₂₀N₂O₂S₂: C, 55.53; H, 6.21; N, 8.63; S, 19.77. Found: C, 55.38; H, 6.32; N, 8.55; S, 19.79.

5.1.44. ***N*-(5-*tert*-Butyl-3,4-dimethyl-1,3-thiazol-2(3*H*)-ylidene)-2-hydroxybenzenesulfonamide (11a).** Under argon atmosphere, boron tribromide (0.17 mL, 1.71 mmol) was added dropwise to a solution of 10f (200 mg, 0.57 mmol) in dichloromethane (20 mL) at −78 °C and stirred at the same temperature for 30 min. The mixture was warmed to room temperature and stirred for 30 min. The reaction mixture was poured into saturated aqueous sodium hydrogen carbonate solution and extracted with chloroform. The organic layer was washed with brine, then dried over anhydrous sodium sulfate. The solvent was removed under reduced pressure and the residue was recrystalized from methanol to give 11a (167 mg, 86%) as a colorless crystals. Mp 201–202 °C. ¹H NMR (DMSO-*d₆*) *δ*: 1.31 (9H, s, CH₃ of *t*-Bu), 2.27 (3H, s, 4-Me), 3.39 (3H, s, 3-Me), 6.93 (1H, dd, *J* = 2.5, 7.8 Hz, benzene), 7.21 (1H, m, benzene), 7.23 (1H, br d, *J* = 7.8 Hz, benzene), 7.31 (1H, t, *J* = 8.3 Hz, benzene), 9.95 (1H, s, OH); FAB-MS *m/z*: 341 (M⁺+1). Anal. Calcd for C₁₅H₂₀N₂O₃·S₂·0.2H₂O: C, 52.36; H, 5.98; N, 8.14; S, 18.64. Found: C, 52.45; H, 5.83; N, 7.94; S, 18.34.

The following compounds were obtained in the same manner.

5.1.45. ***N*-(5-*tert*-Butyl-3,4-dimethyl-1,3-thiazol-2(3*H*)-ylidene)-3-hydroxybenzenesulfonamide (11b).** 87% yield; mp 145–146 °C (diethyl ether–hexane). ¹H NMR (DMSO-*d₆*) *δ*: 1.32 (9H, s, CH₃ of *t*-Bu), 2.27 (3H, s, 4-Me), 3.38 (3H, s, 3-Me), 6.88 (2H, m, benzene), 7.36 (1H, dt, *J* = 1.4, 7.3 Hz, benzene), 7.70 (1H, dd, *J* = 1.4, 7.8 Hz, benzene), 10.12 (1H, s, OH); FAB-MS *m/z*: 341 (M⁺+1). Anal. Calcd for C₁₅H₂₀N₂O₃S₂: C, 52.92; H, 5.92; N, 8.23; S, 18.84. Found: C, 52.78; H, 5.70; N, 8.16; S, 18.84.

5.1.46. ***N*-(5-*tert*-Butyl-3,4-dimethyl-1,3-thiazol-2(3*H*)-ylidene)-4-hydroxybenzenesulfonamide (11c).** 60% yield; mp 234–236 °C (ethyl acetate–hexane). ¹H NMR (DMSO-*d₆*) *δ*: 1.31 (9H, s, CH₃ of *t*-Bu), 1.99 (3H, s, 4-Me), 3.37 (3H, s, 3-Me), 6.84 (2H, d, *J* = 8.6 Hz, benzene), 7.63 (1H, d, *J* = 8.6 Hz, benzene), 10.22 (1H, br s, OH); FAB-MS *m/z*: 341 (M⁺+1). Anal. Calcd for C₁₅H₂₀N₂O₃S₂: C, 52.92; H, 5.92; N, 8.23; S, 18.84. Found: C, 52.68; H, 5.70; N, 8.02; S, 18.45.

5.1.47. ***N*-(5-*tert*-Butyl-3,4-dimethyl-1,3-thiazol-2(3*H*)-ylidene)-3-chloro-2-hydroxybenzenesulfonamide (11d).** 64% yield; mp 147–148 °C (methanol). ¹H NMR (DMSO-*d₆*) *δ*: 1.32 (9H, s, CH₃ of *t*-Bu), 2.29 (3H, s, 4-Me), 3.41 (3H, s, 3-Me), 6.98 (1H, t, *J* = 7.8 Hz, benzene), 7.59 (1H, dd, *J* = 1.5, 7.8 Hz, benzene), 7.69 (1H, dd, *J* = 1.5, 7.8 Hz, benzene), 9.93 (1H, br s, OH); FAB-MS *m/z*: 375 (M⁺+1). Anal. Calcd for C₁₅H₁₉ClN₂O₃S₂: C, 48.05; H, 5.11; N, 7.47; S, 17.11; Cl, 9.46. Found: C, 47.94; H, 5.07; N, 7.32; S, 17.16; Cl, 9.38.

5.1.48. ***N*-(5-*tert*-Butyl-3,4-dimethyl-1,3-thiazol-2(3*H*)-ylidene)-5-chloro-2-hydroxybenzenesulfonamide (11e).** 71% yield; mp 147–149 °C (ethyl acetate–hexane). ¹H NMR (DMSO-*d₆*) *δ*: 1.32 (9H, s, CH₃ of *t*-Bu), 2.28 (3H, s, 4-Me), 3.38 (3H, s, 3-Me), 6.92 (1H, d, *J* = 8.7 Hz, benzene), 7.41 (1H, dd, *J* = 3.0, 8.7 Hz, benzene), 7.65 (1H, d, *J* = 3.0 Hz, benzene), 10.56 (1H, br s, OH); FAB-MS *m/z*: 375 (M⁺+1). Anal. Calcd for C₁₅H₁₉ClN₂O₃S₂: C, 48.05; H, 5.11; N, 7.47; S, 17.11; Cl, 9.46. Found: C, 48.04; H, 5.09; N, 7.61; S, 17.24; Cl, 9.23.

5.1.49. **5-Chloro-*N*-(4-chloro-5-isopropyl-3-methyl-1,3-thiazol-2(3*H*)-ylidene)-2-hydroxybenzenesulfonamide (11f).** 53% yield; mp 132–133 °C (diethyl ether). ¹H NMR (DMSO-*d₆*) *δ*: 1.21 (6H, d, *J* = 6.8 Hz, CH₃ of *i*-Pr), 3.18 (1H, heptet, *J* = 6.8 Hz, CH of *i*-Pr), 3.43 (3H, s, 3-Me), 6.88 (1H, d, *J* = 8.8 Hz, benzene), 7.56 (1H, dd, *J* = 2.4, 8.8 Hz, benzene), 7.79 (1H, d, *J* = 2.4 Hz, benzene), 10.86 (1H, br s, OH); FAB-MS *m/z*: 381 (M⁺+1). Anal. Calcd for C₁₃H₁₄Cl₂N₂O₃S₂: C, 40.95; H, 3.70; N, 7.35; S, 16.82; Cl, 18.60. Found: C, 40.94; H, 3.49; N, 7.36; S, 16.75; Cl, 18.39.

5.1.50. **5-Bromo-*N*-(4-chloro-5-isopropyl-3-methyl-1,3-thiazol-2(3*H*)-ylidene)-2-hydroxybenzenesulfonamide (11g).** 41% yield; mp 135–137 °C (diethyl ether). ¹H

NMR (DMSO-d_6) δ: 1.21 (6H, d, J = 6.8 Hz, CH₃ of *i*-Pr), 3.18 (1H, heptet, J = 6.8 Hz, CH of *i*-Pr), 3.43 (3H, s, 3-Me), 6.93 (1H, d, J = 8.8 Hz, benzene), 7.44 (1H, dd, J = 2.9, 8.8 Hz, benzene), 7.67 (1H, d, J = 2.9 Hz, benzene), 10.85 (1H, br s, OH); FAB-MS *m/z*: 425 (M⁺+1). Anal. Calcd for C₁₃H₁₄ClBrN₂O₃S₂: C, 36.67; H, 3.31; N, 6.58; S, 15.06; Cl, 8.33; Br, 18.77. Found: C, 36.67; H, 3.36; N, 6.54; S, 15.04; Cl, 8.49; Br, 18.53.

5.1.51. 2-Amino-*N*-(5-*tert*-butyl-3,4-dimethyl-1,3-thiazol-2(3*H*)-ylidene)-5-chlorobenzenesulfonamide (12). To a suspension of 10i (960 mg, 2.38 mol) in ethanol (10 mL) and tetrahydrofuran (30 mL) was added 10% palladium–charcoal. The reaction mixture was stirred at room temperature for 1.5 h under hydrogen atmosphere. The suspension was filtered through the Celite pad and evaporated. The residue was purified with recrystalization from isopropanol–diethyl ether to give 12 (548 mg, 62%) as a brown powder. Mp 163–164 °C. ¹H NMR (DMSO-d_6) δ: 1.31 (9H, s, CH₃ of *t*-Bu), 2.27 (3H, s, 4-Me), 3.41 (3H, s, 3-Me), 5.94 (2H, br s, NH2), 6.79 (1H, d, J = 8.8 Hz, benzene), 7.24 (1H, dd, J = 2.4, 8.8 Hz, benzene), 7.49 (1H, d, J = 2.4 Hz, benzene); FAB-MS *m/z*: 374 (M⁺+1). Calcd for C₁₅H₂₀ClN₃O₂S₂: C, 48.18; H, 5.39; N, 11.24; S, 17.15; Cl, 9.48. Found: C, 48.43; H, 5.36; N, 11.10; S, 17.05; Cl, 9.19.

5.1.52. *N*-(2-{[(5-*tert*-Butyl-3,4-dimethyl-1,3-thiazol-2(3*H*)-ylidene)amino]sulfonyl}-4-chlorophenyl)acetamide (13). A solution of 12 (330 mg, 0.88 mmol), *N*,*N*-dimethylaminopyridine (110 mg, 0.88 mmol) and acetyl chloride (0.13 mL, 1.76 mmol) in pyridine (7 mL) was stirred at room temperature for 5 h. The reaction mixture was evaporated and diluted with ethyl acetate. The solution was washed with 1 M hydrochloric acid, saturated aqueous sodium hydrogen carbonate solution and brine, then dried over anhydrous sodium sulfate. The solvent was removed under reduced pressure and the residue was purified by silica gel column chromatography (chloroform–methanol) and recrystalized from acetonitrile to give 13 (92 mg, 25%) as a colorless powder. Mp 194–195 °C. ¹H NMR (DMSO-d_6) δ: 1.28 (9H, s, CH₃ of *t*-Bu), 2.12 (3H, s, 4-Me), 2.28 (3H, s, CH₃ of Ac), 3.41 (3H, s, 3-Me), 7.63 (1H, dd, J = 2.5, 8.8 Hz, benzene), 7.81 (1H, d, J = 2.5 Hz, benzene), 8.11 (1H, d, J = 8.8 Hz, benzene), 9.24 (1H, br s, NH); FAB-MS *m/z*: 416 (M⁺+1). Calcd for C₁₇H₂₂ClN₃O₃S₂: C, 49.09; H, 5.23; N, 10.10; S, 15.42; Cl, 8.52. Found: C, 49.10; H, 5.25; N, 10.06; S, 15.49; Cl, 8.46.

5.1.53. *N*-(5-*tert*-Butyl-3,4-dimethyl-1,3-thiazol-2(3*H*)-ylidene)-5-chloro-2-[(methylsulfonyl)amino]benzenesulfonamide (14). A solution of 12 (200 mg, 0.54 mmol), triethylamine (0.15 mg, 1.08 mmol), and methanesulfonyl chloride (0.062 mL, 0.83 mmol) in tetrahydrofuran (4 mL) was stirred at room temperature for 1 h. The reaction mixture was evaporated and diluted with ethyl acetate. The solution was washed with 1 M hydrochloric acid, saturated aqueous sodium hydrogen carbonate solution and brine, then dried over anhydrous sodium sulfate. The solvent was removed under reduced pres-

sure and the residue was purified by silica gel column chromatography (ethyl acetate–toluene) and recrystalized from methanol to give 14 (135 mg, 56%) as a colorless powder. Mp 165–166 °C. ¹H NMR (DMSO-d_6) δ: 1.32 (9H, s, CH₃ of *t*-Bu), 2.29 (3H, s, 4-Me), 3.24 (3H, s, CH₃ of Ms), 3.44 (3H, s, 3-Me), 7.62 (1H, d, J = 8.8 Hz, benzene), 7.69 (1H, dd, J = 2.4, 8.8 Hz, benzene), 7.82 (1H, d, J = 2.4 Hz, benzene), 8.68 (1H, br s, NH); FAB-MS *m/z*: 452 (M⁺+1). Calcd for C₁₆H₂₂ClN₃O₄S₃: C, 42.51; H, 4.91; N, 9.30; S, 21.28; Cl, 7.84. Found: C, 42.51; H, 4.87; N, 9.29; S, 21.41; Cl, 7.66.

5.1.54. 2-{[(5-*tert*-Butyl-3,4-dimethyl-1,3-thiazol-2(3*H*)-ylidene)amino]sulfonyl}-4-chlorophenyl trifluoromethanesulfonate (15a). A solution of 11e (1.00 g, 2.67 mmol), 2,6-lutidine (0.47 mL, 4.01 mmol), and *N*,*N*-dimethylaminopyridine (33 mg, 0.27 mmol) in dichloromethane (15 mL) was added trifluoromethanesulfonic anhydride (0.68 mL, 4.01 mmol) under ice-bath cooling. The solution was stirred at the same temperature for 30 min. The reaction mixture was poured into water and extracted with chloroform. The organic layer was washed with saturated aqueous potassium hydrogen sulfate and brine, then dried over anhydrous sodium sulfate. The solvent was removed under reduced pressure and the residue was recrystalized from diethyl ether to give 15a (877 mg, 64%) as a colorless powder. This crude product was used for next steps without further purification.

5.1.55. 4-Chloro-2-{[(4-chloro-5-isopropyl-3-methyl-1,3-thiazol-2(3*H*)-ylidene)amino]sulfonyl}phenyl trifluoromethanesulfonate (15b). Compound 15b was obtained from 11f in the same manner as described in the synthesis of 15a quantitative. ¹H NMR (DMSO-d_6) δ: 1.18 (6H, d, J = 6.8 Hz, CH₃ of *i*-Pr), 3.17 (1H, heptet, J = 6.8 Hz, CH of *i*-Pr), 3.48 (3H, s, 3-Me), 7.60 (1H, s, J = 8.8 Hz, benzene), 7.88 (1H, dd, J = 2.4, 8.8 Hz, benzene), 8.01 (1H, d, J = 2.4 Hz, benzene); FAB-MS *m/z*: 513 (M⁺+1).

5.1.56. Methyl 2-{[(5-*tert*-butyl-3,4-dimethyl-1,3-thiazol-2(3*H*)-ylidene)amino]sulfonyl}-4-chlorobenzoate (16). Under argon atmosphere, 15a (25.4 g, 50.1 mmol) was dissolved in *N*,*N*-dimethylformamide (280 mL) and methanol (140 mL). Triethylamine (12.9 mL, 92.6 mmol), 1,3-bis(diphenylphosphino)propane (1.74 g, 4.2 mmol), palladium acetate (0.95 g, 4.2 mmol) was added and carbon monoxide gas was bubbled. The reaction mixture was stirred at 70 °C for 2.5 h under carbon monoxide atmosphere. The mixture was evaporated and diluted with ethyl acetate. The organic layer was washed with 1 M hydrochloric acid and brine, then dried over anhydrous sodium sulfate. The solvent was removed under reduced pressure and the residue was purified by silica gel column chromatography (ethyl acetate–toluene) and recrystalized from isopropanol–diethyl ether to give 16 (7.32 g, 42%) as a colorless powder. Mp 142–143 °C. ¹H NMR (DMSO-d_6) δ: 1.32 (9H, s, CH₃ of *t*-Bu), 2.30 (3H, s, 4-Me), 3.43 (3H, s, 3-Me), 3.78 (3H, s, CH₃ of COOMe), 7.61 (d, J = 8.3 Hz, benzene), 7.75 (1H, dd, J = 2.0, 8.3 Hz, benzene), 7.91 (1H,

d, $J = 2.0$ Hz, benzene); FAB-MS m/z: 417 (M$^+$+1).
Calcd for C$_{17}$H$_{21}$ClN$_2$O$_4$S$_2$: C, 48.97; H, 5.08; N, 6.72;
S, 15.38; Cl, 8.50. Found: C, 49.02; H, 4.95; N, 6.78;
S, 15.43; Cl, 8.47.

5.1.57. 2-{[(5-*tert*-Butyl-3,4-dimethyl-1,3-thiazol-2(3*H*)-ylidene)amino]sulfonyl}-4-chlorobenzamide (17a). To a
solution of 16 (100 mg, 0.248 mmol) in *N,N*-dimethyl-
formamide (2 mL), 1-hydroxybenzotriazole (50 mg,
0.372 mmol), 1-[3-(dimethylamino)propyl]-3-ethylcar-
bodiimide   hydrochloride   (WSC·HCl,   71 mg,
0.372 mmol), *N,N*-diisopropylethylamine (0.17 mL,
0.992 mmol), and ammonium chloride (27 mg,
0.496 mmol) was added. The solution was stirred at
room temperature for 2.5 h. The reaction mixture was
poured into water and extracted with chloroform. The
organic layer was washed with 1 M hydrochloric acid
and brine, then dried over anhydrous sodium sulfate.
The solvent was removed under reduced pressure and
the residue was purified by silica gel column chromato-
graphy (methanol–chloroform) and recrystalized from
diethyl ether to give 17a (71 mg, 71%) as a colorless
powder. Mp 196–198 °C. ^{1}H NMR (DMSO-d_6) δ: 1.31
(9H, s, CH$_3$ of *t*-Bu), 2.28 (3H, s, 4-Me), 3.42 (3H, s,
3-Me), 7.47 (1H, d, $J = 8.3$ Hz, benzene), 7.61 (2H, br
s, NH$_2$), 7.68 (1H, dd, $J = 2.0$, 8.3 Hz, benzene), 7.87
(1H, d, $J = 2.0$ Hz, benzene); FAB-MS m/z: 402
(M$^+$+1). Anal. Calcd for C$_{16}$H$_{20}$ClN$_3$O$_3$S$_2$: C, 47.81;
H, 5.02; N, 10.45; S, 15.96; Cl, 8.82. Found: C, 47.72;
H, 4.78; N, 10.42; S, 15.82; Cl, 8.91.

**5.1.58.   4-Cyano-2-{[(5-isopropyl-3,4-dimethyl-1,3-thi-
azol-2(3*H*)-ylidene)amino]sulfonyl}benzamide (17b).** Com-
pound 17b was obtained from 10q in the same manner as
described in the synthesis of 17a. 68% yield. ^{1}H NMR
(DMSO-d_6) δ: 1.15 (6H, d, $J = 6.8$ Hz, CH$_3$ of *i*-Pr),
2.17 (3H, s, 4-Me), 3.21 (1H, heptet, $J = 6.8$ Hz, CH of
i-Pr), 3.43 (3H, s, 3-Me), 7.61 (1H, d, $J = 8.3$ Hz, ben-
zene), 7.72 (2H, br d, $J = 6.3$ Hz, NH$_2$), 8.02 (1H, dd,
$J = 1.9$ Hz, benzene), 8.27 (1H, d, $J = 1.9$ Hz, benzene);
FAB-MS m/z: 379 (M$^+$+1).

**5.1.59. 2,5-Dicyano-*N*-(5-isopropyl-3,4-dimethyl-1,3-thi-
azol-2(3*H*)-ylidene)benzenesulfonamide (18b).** Phospho-
rous   oxychloride   (0.3 mL,   3.3 mmol)   and   *N,N*-
dimethylformamide (50 μL, 0.66 mmol) was added to a
solution of 17b (250 mg, 0.66 mmol) in chloroform
(30 mL). The reaction mixture was refluxed for 24 h.
The reaction mixture was poured into ice-water and ex-
tracted with chloroform. The organic layer was washed
with saturated aqueous sodium hydrogen carbonate and
brine, then dried over anhydrous sodium sulfate. The
solvent was removed under reduced pressure and the
residue was purified by silica gel column chromatogra-
phy (methanol–chloroform) to give 18b (52 mg, 22%)
as a yellow powder. Mp 222–224 °C. ^{1}H NMR
(DMSO-d_6) δ: 1.15 (6H, d, $J = 6.8$ Hz, CH$_3$ of *i*-Pr),
2.19 (3H, s, 4-Me), 3.22 (1H, heptet, $J = 6.8$ Hz, CH
of *i*-Pr), 3.49 (3H, s, 3-Me), 8.28 (2H, m, benzene),
8.42 (1H, br s, benzene); FAB-MS m/z : 361 (M$^+$+1).
Anal. Calcd for C$_{16}$H$_{16}$N$_4$O$_2$S$_2$: C, 53.31; H, 4.47; N,
15.54; S, 17.79. Found: C, 53.15; H, 4.39; N, 15.70; S,
17.74.

**5.1.60.   *N*-(5-*tert*-Butyl-3,4-dimethyl-1,3-thiazol-2(3*H*)-
ylidene)-5-chloro-2-cyanobenzenesulfonamide   (18a).**
Compound 18a was obtained from 17a in the same man-
ner as described in the synthesis of 18b. 67% yield; mp
160–162 °C. ^{1}H NMR (DMSO-d_6) δ: 1.32 (9H, s, CH$_3$
of *t*-Bu), 2.30 (3H, s, 4-Me), 3.49 (3H, s, 3-Me), 7.88
(1H, ·dd, $J = 2.0$, 8.3 Hz, benzene), ·8.02 (1H, d,
$J = 2.0$ Hz, benzene), 8.09 (1H, d, $J = 8.3$ Hz, benzene);
FAB-MS m/z: 384 (M$^+$+1). Anal. Calcd for
C$_{16}$H$_{18}$ClN$_3$O$_2$S$_2$: C, 50.06; H, 4.73; N, 10.95; S, 16.70;
Cl, 9.23. Found: C, 49.84; H, 4.63; N, 10.75; S, 16.67;
Cl, 9.15.

**5.1.61.   5-Chloro-*N*-(4-chloro-5-isopropyl-3-methyl-1,3-
thiazol-2(3*H*)-ylidene)-2-cyanobenzenesulfonamide   (19).**
Under argon atmosphere, 15b (3.64 g, 7.1 mmol) was
dissolved in *N,N*-dimethylformamide (100 mL) and pal-
ladium tris(dibenzylideneacetone)dipalladium (408 mg,
0.71 mmol), 1,1′-bis(diphenylphosphino)ferrocene (787
mg, 14.2 mmol), zinc powder (56 mg, 0.85 mmol), and
zinc(II) cyanide (500 mg, 4.3 mmol) was added. The
reaction mixture was stirred at 130 °C for 2.5 h under
argon atmosphere. The mixture was evaporated and
diluted with ethyl acetate. The organic layer was
washed with 2 M aqueous ammonia solution, water,
and brine, then dried over anhydrous sodium sulfate.
The solvent was removed under reduced pressure and
the residue was purified by silica gel column chromato-
graphy (ethyl acetate–toluene) and recrystalized from
isopropanol to give 19 (1.38 g, 50%) as a pale yellow
powder. Mp 181–182 °C (isopropanol). ^{1}H NMR
(DMSO-d_6) δ: 1.20 (6H, d, $J = 6.8$ Hz, CH$_3$ of *i*-Pr),
3.18 (1H, heptet, $J = 6.8$ Hz, CH of *i*-Pr), 3.32 (3H,s,
3-Me), 7.92 (1H, dd, $J = 1.9$, 8.3 Hz, benzene), 8.04
(1H, d, $J = 1.9$ Hz, benzene), 8.12 (1H, d, $J = 8.3$ Hz,
benzene); FAB-MS m/z: 390 (M$^+$+1). Anal. Calcd for
C$_{14}$H$_{13}$Cl$_2$N$_3$O$_2$S$_2$: C, 43.08; H, 3.36; N, 10.77; S,
16.43; Cl, 18.17. Found: C, 43.03; H, 3.23; N, 10.70; S,
16.34; Cl, 18.21.

**5.1.62.   *N*-(4-Chloro-5-isopropyl-3-methyl-1,3-thiazol-
2(3*H*)-ylidene)-2,5-dicyanobenzenesulfonamide   (20).**
Compound 20 was obtained from 15b in the same man-
ner as described in the synthesis of 19 with 1.6 mol equiv
of Zn(CN)$_2$. 60% yield. Mp 205–207 °C (isopropanol).
^{1}H NMR (CDCl$_3$): 1.27 (6H, d, $J = 6.8$ Hz, CH$_3$ of *i*-
Pr), 3.22 (1H, heptet, $J = 6.8$ Hz, CH of *i*-Pr), 3.60
(3H, s, 3-Me), 7.87 (1H, dd, $J = 1.9$, 8.3 Hz, benzene),
7.92 (1H, d, $J = 8.3$ Hz, benzene), 8.47 (1H, d,
$J = 1.9$ Hz, benzene); FAB-MS m/z: 381 (M$^+$+1). Anal.
Calcd for C$_{15}$H$_{13}$ClN$_4$O$_2$S$_2$: C, 47.30; H, 3.44; N,
14.71; S, 16.84; Cl, 9.31. Found: 47.15; H, 3.52; N,
15.00; S, 16.65; Cl, 9.35.

5.2. Pharmacology

5.2.1. In vitro RT inhibition assay. A expression plas-
mide, pG280, encoding HIV-1 RT proteins as LacZ fu-
sion proteins were used for the expression of the WT RT
and mutated RTs.[12] The single amino acid-substituted
RTs (K103N RT and Y181C RT) were constructed
using pG280 from a Quikchange™ Site-Directed Muta-
genesis Kit (Stratagene, La Jolla, CA). Recombinant